Vascular regeneration was augmented in AM-Tg mice after 20m-MCAO associated with increased mobilization of CD34$^+$ mononuclear cells

The blood flow in the ischemic brain estimated by LDPI was significantly higher in AM-Tg mice after postoperative d 7 and higher flow was maintained until d 56. The brain blood flow ratio (ipsilateral/contralateral, %) on d 56 was 88.9 ± 2.8 in Wt *vs.* 97.6 ± 3.0 in AM-Tg ($P < 0.01$ by ANCOVA; n = 8; Fig. 4, C, D, and H). We were also able to confirm that capillary density determined as the number of PECAM-1$^+$ cells was augmented in AM-Tg mice. The density (/mm^2) on d 56 was 468.8 ± 21.8 in Wt *vs.* 536.6 ± 13.6 in AM-Tg ($P < 0.05$; n = 8; Fig. 4I). Thus, the physiological neovascularization in the ischemic core after stroke was augmented in AM-Tg mice. Peripheral CD34$^+$ mononuclear cells were physiologically enhanced after 20m-MCAO and further increased in AM-Tg mice on d 3–7. The cells (/ml) on d 3 numbered 1774 ± 272 in Wt *vs.* 3199 ± 562 in AM-Tg ($P < 0.05$; n = 6; Fig. 5, A–C).

Augmented neurogenesis and improved recovery of impaired neurological function were observed in AM-Tg mice after 20m-MCAO

BrdU injection on postoperative d 4~6 proved that most BrdU-positive cells were costained with GFAP (data not shown) and that there were far fewer BrdU-PECAM-1 or BrdU-NeuN double-positive cells. We found that regenerated neurons defined as BrdU-NeuN double-positive cells were frequently detected adjacent to the vasculature and the number of these cells on d 56 was correlated with capillary density ($P = 0.003$; n = 12; Fig. 6, A and B; and Table 2). The cells increased from postoperative d 7–56, and their number was significantly higher in AM-Tg mice. The regenerated neurons (/mm^2) on d 56 numbered 20.4 ± 3.9 in Wt *vs.* 33.9 ± 4.7 in AM-Tg ($P < 0.05$; n = 12; Fig. 6C).

Recovery of impaired motor function after 20m-MCAO, quantified as the exercise time on an accelerating rota-rod from the start to collapse down, was significantly better in AM-Tg mice. The exercise time (second) on d 49 was 21.5 ± 1.5 for Wt *vs.* 27.1 ± 2.0 for AM-Tg ($P < 0.01$ by ANCOVA; n = 14; Fig. 6D). To confirm whether vasculogenesis and neurogenesis are the contributing factor to the recovery from the ischemic damage, we analyzed the relation between capillary density, the number of regenerated neuron and the rota-rod result in AM-Tg mice after 20m-MCAO. As shown in Table 2, we found that the capillary density was significantly correlated with the rota-rod exercise time ($P = 0.005$; n = 24) and neurogenesis tended to be correlated with it ($P = 0.08$; n = 12).

Low-concentration AM-Tg mice also showed reduced infarct area and promoted vascular regeneration

We performed 20m-MCAO, using the low-concentration AM-Tg mice (plasma mature AM, 2.6 ± 0.6 fmol/ml) as well as the high-concentration line (plasma mature AM, 24.9 ± 4.2 fmol/ml) to determine appropriate concentration for AM

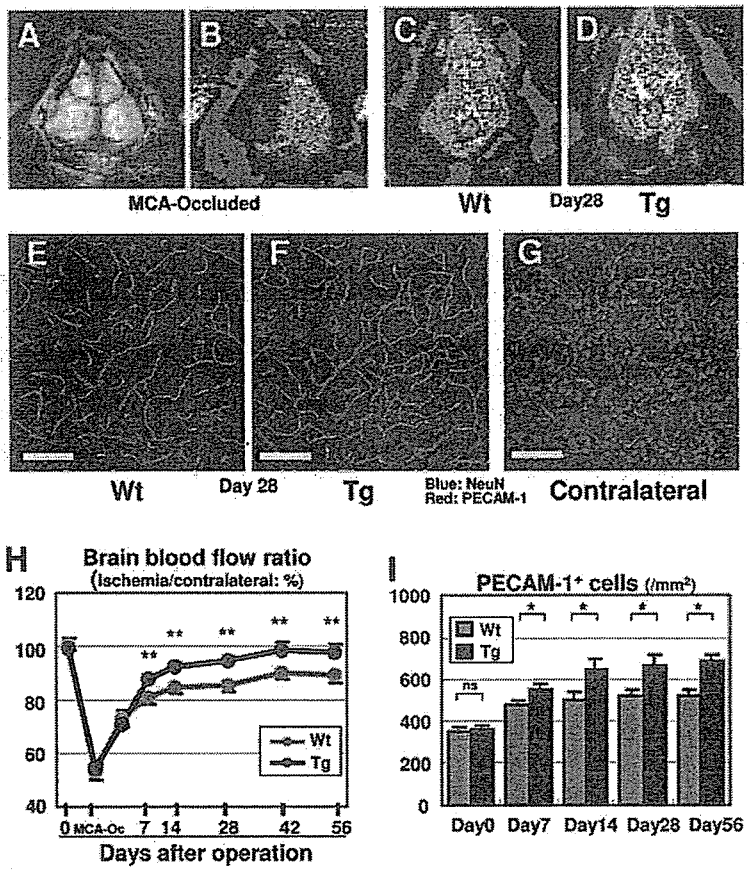

FIG. 4. Effects of AM on vascular regeneration in the ischemic brain after 20m-MCAO. A–D, Analysis of the blood flow in the ischemic brain by LDPI evaluated in mice with the scalp removed (A). Flowmetric analysis of the ischemic brain during MCA-Occlusion (B) and on d 28 after 20m-MCAO in Wt (C) and AM-Tg (D). *Red* or *white* indicates higher flow than *blue* or *green*. E–G, Histological examination of the vasculature in the ischemic core with PECAM-1 staining. Ischemic striatum on d 28 after 20m-MCAO in Wt (E) and AM-Tg (F), and contralateral nonischemic striatum (G). *Scale bar*, 100 μm (×20 magnification). H, Quantitative analysis of the blood flow in the ischemic brain. Comparison of recovery from ischemia after 20m-MCAO between Wt and AM-Tg. MCA-Oc, blood flow during MCA occlusion; **, $P < 0.01$ for Wt *vs.* AM-Tg by ANCOVA; n = 8. I, Quantitative analysis of capillary density in the ischemic brain. Comparison of time course for increase in capillary density, determined as the number of PECAM-1$^+$ cells, between Wt and AM-Tg mice. *, $P < 0.05$; ns, not significant; n = 8.

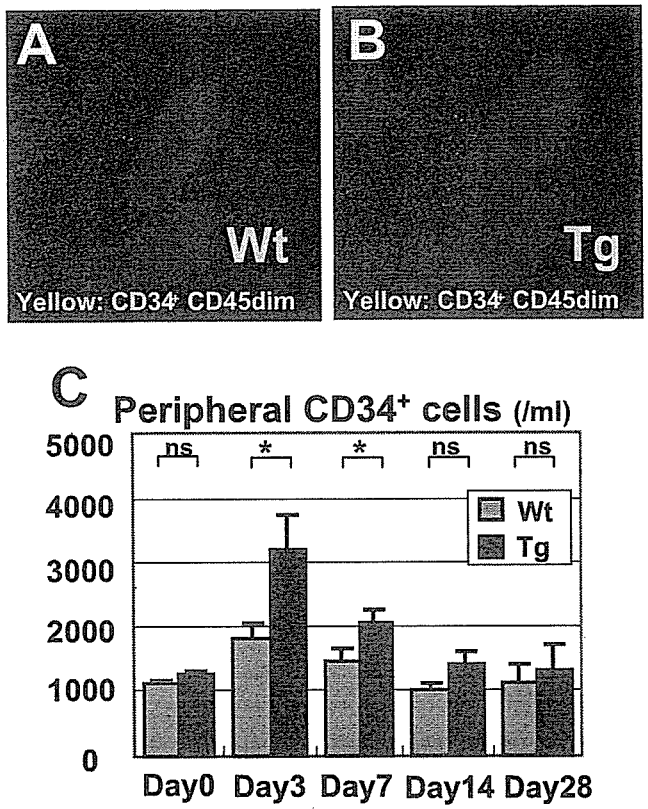

FIG. 5. Effects of AM on mobilization of $CD34^+$ mononuclear cells into peripheral blood after 20m-MCAO. A–C, Quantification of $CD34^+$ mononuclear cells after 20m-MCAO. Scatter plots for fluorescence-activated cell sorting analysis of the $CD34^+$ cells in peripheral blood of Wt (A) and AM-Tg (B) on postoperative d 3. *Yellow*, $CD34^+$-CD45dim mononuclear cells. Comparison of the time course for mobilization of $CD34^+$ cells into peripheral blood between Wt and AM-Tg (C). *, $P < 0.05$; ns, not significant; n = 6.

treatment. The result showed comparable levels of neuroprotection and vascular regeneration between the low-concentration line and the high-concentration line (Table 3). We further analyzed BP-matched mice by administration of low-dose hydralazine (0.1 mM in drinking water) to exclude the possibility that lower BP observed in AM-Tg mice caused beneficial effects after 20m-MCAO. As shown in Table 3, lower BP alone did not reduce the infarct area nor promote vascular regeneration, although hydralazine administration caused BP reduction comparable to that in AM-Tg mice.

Brain edema was reduced in AM-Tg mice at 24 h after 2 h MCAO

The survival rate of mice after the fatal stroke, 2 h-MCAO, was 0% on d 7. We observed no significant difference in the rate between Wt and AM-Tg mice. The edema volume was reduced in AM-Tg mice 24 h after 2 h-MCAO; although the infarct volume showed no significant difference between them. Edema volume (% volume of contralateral hemisphere) was 13.5 ± 1.2 in Wt *vs.* 9.7 ± 0.9 in AM-Tg ($P < 0.05$; n = 9, Fig. 7C), whereas infarct volume (% volume of contralateral hemisphere) was 39.0 ± 4.9 in Wt *vs.* 44.5 ± 7.3 in AM-Tg (not significant; n = 9; Fig. 7, A and B). As shown in Fig. 7D, we found that Evans Blue leakage into the ischemic

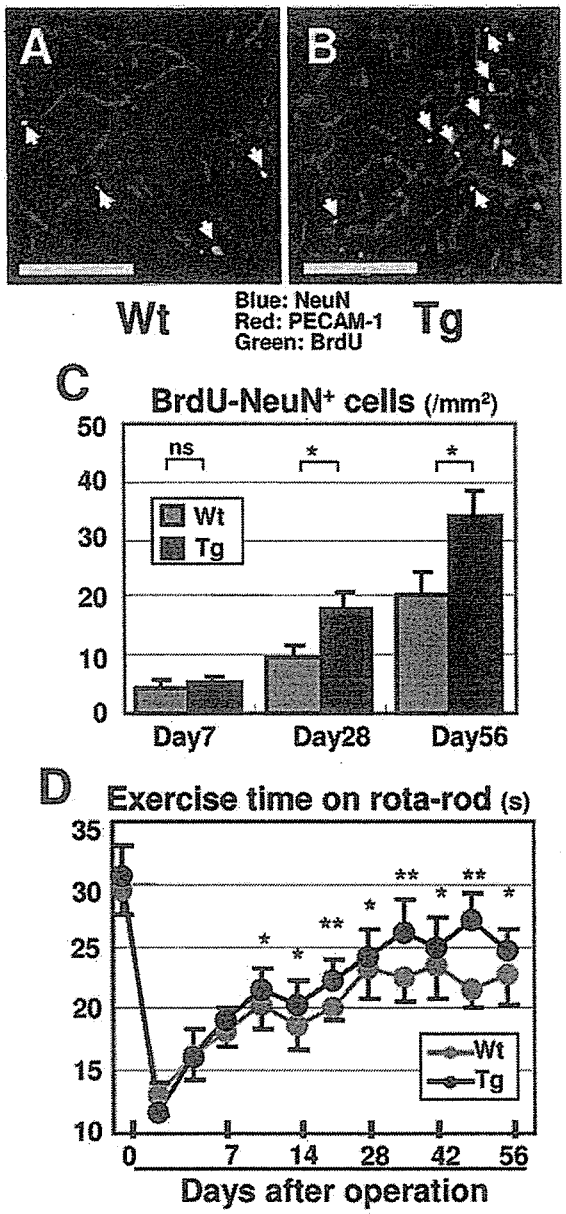

FIG. 6. Effects of AM on neurogenesis and recovery of impaired motor function after 20m-MCAO. A and B, Detection of regenerated neurons on postoperative d 56 by immunostaining for BrdU and NeuN. *Arrows*, BrdU-NeuN double-positive cells in the ischemic core of Wt (A) and AM-Tg (B). *Scale bar*, 100 μm. C, Quantitative analysis of regenerated neurons. *, $P < 0.05$; ns, not significant; n = 12. D, Recovery of impaired motor function after 20m-MCAO, quantified as the exercise time on an accelerating rota-rod from the start to collapse down. *, $P < 0.05$; **, $P < 0.01$ for Wt *vs.* AM-Tg by ANCOVA; n = 14.

core was significantly reduced in AM-Tg mice. The content of Evans Blue (ng/g tissue) in the ischemic brain at 24 h after 2 h-MCAO was 239.4 ± 37.3 in Wt *vs.* 133.9 ± 9.4 in AM-Tg ($P < 0.01$; n = 4; Fig. 7E).

AM exerted direct antiapoptotic and neurodifferentiating effects on neuronal cells in vitro

After 48 h incubation of NHNP under serum-free apoptotic conditions, in which the number of the cells had decreased

TABLE 2. Significant correlation between the regenerative elements and apoptosis, neurogenesis, and functional recovery after 20m-MCAO

X	Y	Regression line	*P*
Capillary density (% field)	Apoptotic cells (/mm^2)	Y = −2.3X+37	0.01
Capillary density (% field)	Regenerated neuron (/mm^2)	Y = 3.2X-21	0.003
Capillary density (% field)	Rota-rod result (sec)	Y = 1.3X+9	0.005
Regenerated neuron (/mm^2)	Rota-rod result (sec)	Y = 0.3X+19	0.08

n = 12–24.

to half, the viable cell number was increased in the AM 10^{-8} mol/liter-treated group to 38.8 ± 7.1% over the control ($P < 0.01$; n = 4; Fig. 8C). The ratio of ssDNA$^+$ cells to total cells (%) was 9.8 ± 1.9 in Wt *vs.* 4.0 ± 0.6 in the AM 10^{-8} mol/liter-treated group ($P < 0.05$; n = 4; Fig. 8, A, B, and D).

After 7-d incubation of PC12 cells under differentiation condition, both the cell number and the length of neuronal process increased dose dependently as a result of AM treatment ($P < 0.01$; n = 6; Fig. 8, E and I). Coculture with endothelial cells also increased the cell number and the length of neuronal process. The effect of AM was canceled by AM blockers, PKA inhibitors, and PI3K inhibitors (Table 4).

Exogenous administration of AM reduced infarct area, promoted vascular regeneration, and improved neurological function after 20m-MCAO

We further examined the effects of exogenous infusion of mature AM by means of an osmotic pump in the amount reported to achieve a plasma concentration of 2 fmol/ml. Implantation of the pump just after the operation resulted in increase in the blood flow and reduction of the infarct area on postoperative d 7 to a comparable level to those in AM-Tg mice. Moreover, the treatment started at 24 h after the operation (d 1) showed almost the same therapeutic effect. However, the implantation at 72 h after the operation (d 3) failed to reveal any significant effect (Fig. 9, A and B). The rota-rod exercise time was significantly improved in the AM-treated group. The exercise time (second) on d 7 was 17.0 ± 1.5 in vehicle group *vs.* 18.1 ± 2.0 in AM-treated group (n = 6 for vehicle group and 12 for AM-treated group; $P < 0.05$ by ANCOVA).

Discussion

In the present study, we generated novel transgenic mice that overproduce AM in their liver without overproduction of mature PAMP and investigated the roles of AM in degeneration or regeneration processes after brain ischemia, which can be defined as brain remodeling, as summarized in Fig. 10. Brain edema in acute phase, neuronal loss and gliosis in subacute to chronic phase after 20m-MCAO were reduced in AM-Tg mice. Furthermore, vascular regeneration, mobilization of CD34$^+$ mononuclear cells and subsequent neurogenesis were enhanced in them. These effects resulted in improved recovery of motor function after the nonfatal stroke. AM was also found to exert direct antiapoptotic and neuro-differentiating effects on neuronal cells *in vitro*. Exogenous administration of AM in mice after 20m-MCAO also

TABLE 3. Comparison of the effects on neuroprotection and vascular regeneration after 20m-MCAO between Wt control mice, hydralazine-administrated mice, and the low and high concentration lines of AM-Tg

Mice	Infarct area (mm^2/field)	Brain blood flow (% Contralateral)	Systolic BP (mm Hg)
Control	0.90 ± 0.09	80.8 ± 2.3	120.1 ± 2.2
Hydralazine	0.94 ± 0.17^{ns}	79.6 ± 2.6^{ns}	101.0 ± 3.9^a
Low-conc. AM-Tg	0.58 ± 0.12^b	88.4 ± 2.9^b	105.1 ± 1.8^a
High-conc. AM-Tg	0.67 ± 0.09^b	86.3 ± 2.0^b	106.4 ± 3.5^a

conc., Concentration.
$^a P < 0.01$; $^b P < 0.05$; ns, not significant *vs.* control; n = 6.

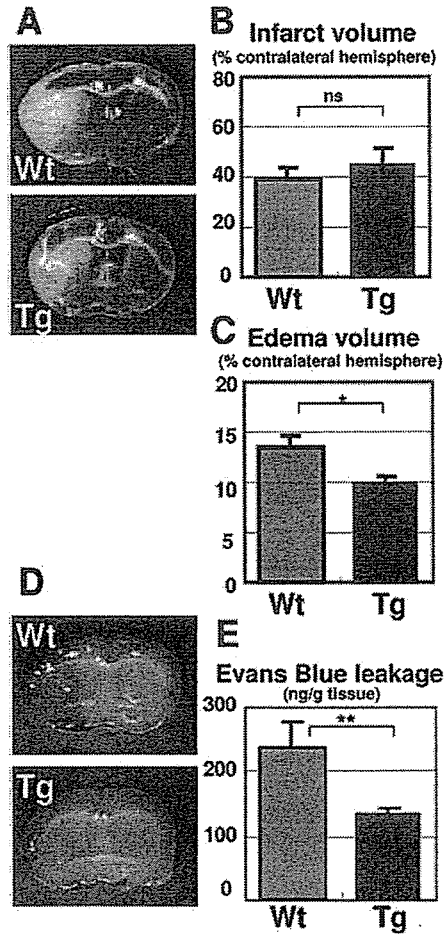

FIG. 7. Effects of AM on infarct size and brain edema in the fatal stroke, 2 h-MCAO. A, Comparison of infarct size between Wt and AM-Tg with 2,3,5-triphenyltetrazolium chloride staining at 4.0 mm from the frontal pole. *White area* represents infarction. B and C, Infarct (B) and edema (C) volumes quantified 24 h after the operation of 2 h-MCAO. *, $P < 0.05$; ns, not significant for Wt and AM-Tg; n = 9. D: Representative image of *in situ* Evans Blue leakage into the ischemic core at 24 h after 2 h-MCAO. E, Quantification of Evans Blue in the ischemic brain. **, $P < 0.01$; n = 4.

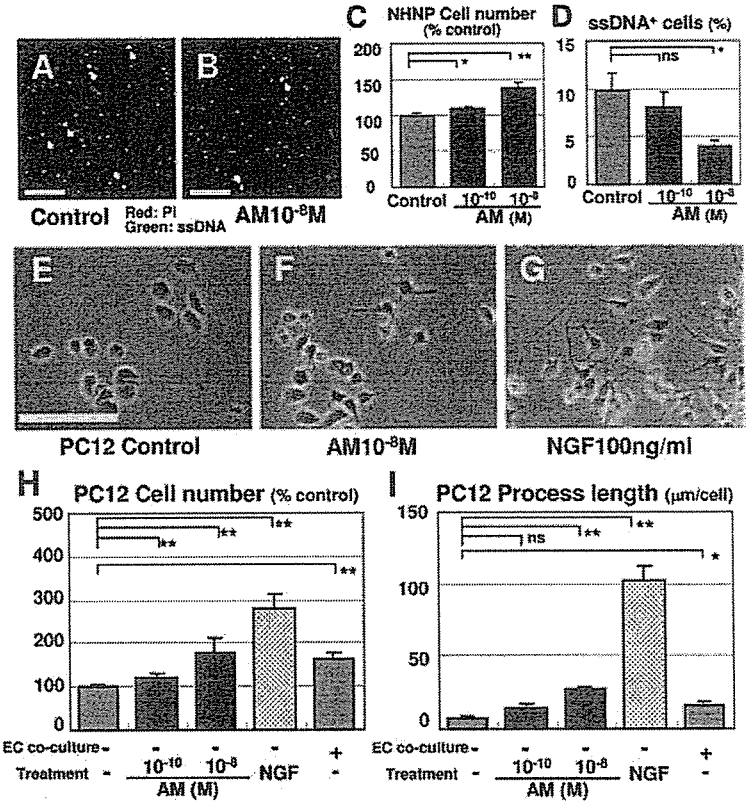

FIG. 8. Effects of AM *in vitro* on apoptosis of NHNP neuronal progenitor cells and neuronal differentiation of PC12 cells. A–D, *In vitro* analysis of apoptotic NHNP after incubation with (B) or without (A) AM. NHNP cell number (C) and the ratio of ssDNA$^+$ cells to total cells (D) after 48 h incubation. *, $P < 0.05$; **, $P < 0.01$; ns, not significant *vs.* control; n = 4; *scale bar*, 100 μm. E–G, Effects of AM on neuronal differentiation of PC12 cells evaluated by the length of neuronal process. Microscopic examination of PC12 cells after incubation for 7 d (E). AM (F) or nerve growth factor (G) was added to the culture medium. Quantification of cell number (H) and the length of neuronal process (I). *, $P < 0.05$; **, $P < 0.01$; ns, not significant; n = 6; *scale bar*, 100 μm.

reduced the infarct area, and promoted vascular regeneration and functional recovery.

Stroke causes two different types of neuronal death: necrosis and apoptosis. Acute neuronal loss, which is completed within a few days after ischemic damage, is necrotic, whereas delayed neuronal loss, which may start several days after transient ischemia, is considered to be apoptotic (27, 28). Many studies have found that treatments that reduce inflammation or oxidative stress are beneficial for the prevention of apoptotic neuronal loss (29, 30).

In this study, we demonstrated that AM exerts neuroprotective actions in the ischemic brain. A significant reduction in neuronal loss in AM-Tg mice after 20m-MCAO became obvious after postoperative d 7, but was not obvious before d 3. A significant decrease in ssDNA-positive cells inside and on the border of the ischemic area was observed in AM-Tg mice in association with a reduction in CD45$^+$ cells and *in situ* ROS production in the subacute phase. AM is therefore assumed to reduce delayed neuronal loss through suppression of the apoptotic process. Furthermore, we confirmed that AM directly suppresses apoptosis of neuronal progenitor cells *in vitro*. These findings suggest that AM exerts neuroprotective effects on the ischemic brain by reducing apoptotic neuronal loss through both its direct antiapoptotic action on neurons and indirect effect via antiinflammation and anti-ROS production. Consistent with the findings in this study, several recent reports have provided evidences for the organ-protective effects of AM against inflammation and oxidative stress (31–33). In addition, we found significant negative correlation between capillary density and apoptotic cells in the same section on postoperative d 7 after 20m-MCAO. Moreover, the infarct area kept expanding between d 7–28 in Wt mice, whereas AM-Tg mice did not show the increase in size in this period. These findings suggest that the increased blood flow in AM-Tg mice was one of the causes of neuroprotection after 20m-MCAO, although we suppose that multiple actions of AM, as described above, could also contribute for neuroprotection.

Increased vascularity is reported to be associated with improved neurological recovery in human patients with stroke (34). This implies that physiological vascular regeneration in the ischemic brain constitutes a beneficial response for the recovery of impaired neurological function. Moreover, neurogenesis after stroke even in adulthood has been demonstrated to occur in a place surrounded by the vascu-

TABLE 4. Effects of AM-antagonists, PKA inhibitors, and PI3K inhibitors on AM-induced neural differentiation of PC12 cells

	Process length (μm/cell)
PC12	6.8 ± 1.7
+AM (10^{-8} mol/liter)	23.6 ± 4.0[a]
+AM+AM(22–52) (10^{-5} mol/liter)	11.8 ± 3.4[b]
+AM+CGRP(8–37) (10^{-5} mol/liter)	14.8 ± 1.9[c]
+AM+Rp-cAMP (10^{-5} mol/liter)	10.2 ± 2.7[b]
+AM+PKA Inh (10^{-6} mol/liter)	7.2 ± 2.3[b]
+AM+LY294002 (10^{-5} mol/liter)	4.6 ± 1.6[b]
+AM+wortmannin (10^{-7} mol/liter)	5.4 ± 1.1[b]
PC12-EC coculture	20.7 ± 2.1[a]

EC, Endothelial cell.

[a] $P < 0.01$ *vs.* PC12 without AM; [b] $P < 0.01$ *vs.* PC12 with AM (10^{-8} mol/liter); [c] $P < 0.05$; n = 8.

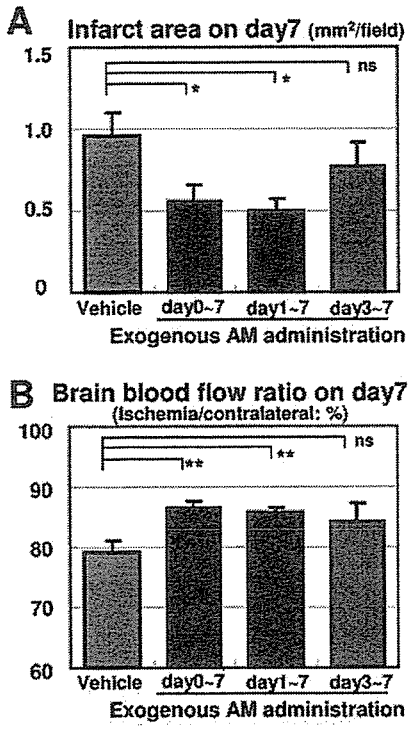

FIG. 9. Effects of exogenously administrated AM on neuroprotection and vascular regeneration after 20m-MCAO. 50 ng/h AM was administrated to mice with an ip implanted osmotic pump. Infarct area (A) and blood flow (B) on postoperative d 7 with different starting points for AM administration. *, $P < 0.05$; **, $P < 0.01$; ns, not significant *vs.* vehicle; n = 6.

lature, the so-called "vascular niche" (35), where endothelial cells secrete neurogenic factors, including basic fibroblast growth factor, vascular endothelial growth factor, and brain-derived neurotrophic factor, and create conditions conducive to neurogenesis (36). Therefore, vascular regeneration is assumed to rescue ischemic brain via not only supply of oxygen and nutrition but also promotion of neurogenesis. We confirmed in this study that neurogenesis occurred adjacent to neovessels in the ischemic core and the number of regenerated neurons was correlated with vascular density.

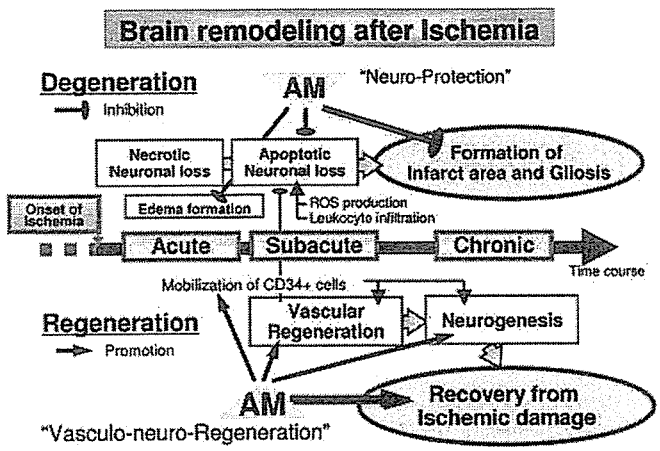

FIG. 10. Summary of brain remodeling after ischemia and effects of AM on the ischemic brain observed in this study.

We have assigned the term "vasculo-neuro-regeneration" to the entire process of enhancement of vasculogenesis and subsequent neurogenesis.

We demonstrated that AM promotes vasculo-neuro-regeneration in the ischemic brain. Blood flow and capillary density in the ischemic brain after 20m-MCAO was significantly enhanced in AM-Tg mice after postoperative d 7 with subsequent promotion of neurogenesis after d 28. The promoted vasculogenesis and neurogenesis observed in AM-Tg mice was significantly correlated with the functional recovery after 20m-MCAO. This result suggests that these two regenerative elements might contribute to the functional recovery after 20m-MCAO. The neovascularization was preceded by augmented mobilization of $CD34^+$ mononuclear cells, which are known to differentiate into endothelial cells and contribute to vasculogenesis (37). Recently, iv infusion of $CD34^+$ cells has reported to promote not only neovascularization but also neurogenesis (38). Furthermore, we observed the direct promoting action of AM on neural differentiation of PC12 cells via cAMP/PKA- and PI3K/Akt-dependent pathways. The totality of these findings suggests that the neurogenic action of AM *in vivo* comprises at least two different mechanisms: a direct action on neuronal cells through activation of PKA and Akt and an indirect action on neurogenesis after enhanced neovascularization.

Judging from the ratio of mature AM to total AM as shown in Table 1, the mature AM concentration in the ischemic brain of AM-Tg mice was expected to be 1~4 fmol/g tissue. The concentration seems to be comparable to the reported effective concentration of mature AM *in vivo* (25, 39). The *in vivo* concentration of human mature AM in the whole brain (1 fmol/g tissue level) and in the plasma (10 fmol/ml level) might be lower than the minimal concentration required for its *in vitro* action (100 fmol/ml) observed in this study. The actual effective concentration *in vitro*, however, might be lower because the administrated peptide is rapidly degradated *in vitro*. In addition, it is demonstrated in previous reports including ours (40, 41), that peptides could exert their significant actions at the stably maintained concentration, that is, by 2 orders of magnitude lower than that of bolus administration. In AM-Tg mice, the AM concentration was maintained at the same level due to the constitutive overproduction by the human serum amyloid P component promoter. Thus, we suppose that the direct neuronal action of AM *in vivo* could be possible in this stroke model.

In view of clinical application, we also tried exogenous administration of AM by ip implanted osmotic pump to determine appropriate amount and timing of AM administration after 20m-MCAO. Previous reports on AM administration for rodents or human set the therapeutic dose at 2~25 fmol/ml (25, 39). For our experiments, therefore, we used two lines of transgenic mice with a plasma concentration of mature AM of 24.9 ± 4.2 and 2.6 ± 0.6 fmol/ml. The results showed comparable effects of AM in these two lines on neuroprotection and vascular regeneration. This led us to conclude that a plasma level of 2~3 fmol/ml of mature AM, 3~5 times higher than its physiological concentration, was sufficient to attain therapeutic effects for the mice after 20m-MCAO. We next tried exogenous infusion of AM with an osmotic pump in the amount reported to achieve a plasma

concentration of 2~3 fmol/ml. The exogenous AM treatment which started just after the induction of 20m-MCAO or at 24 h after produced significant effects that were comparable to those seen in the two lines of AM-Tg mice. However, that from 72 h postoperatively failed to reveal significant effects. These results showed that appropriate timing to start AM administration after stroke is less than 72 h after the event.

We performed two different stroke models, nonfatal 20m-MCAO and fatal 2 h-MCAO. In 2 h-MCAO, we observed significant reduction of brain edema in AM-Tg mice through reduction of vascular permeability, which is compatible with previous report (42). However, infarct size was not reduced on postoperative d 1 after 2 h-MCAO. The result suggests that AM exerts more significant therapeutic effect on the brain tissue after nonfatal ischemia. The therapeutic potential for brain edema after fatal stroke is further to be elucidated.

Cerebral ischemia, including stroke, vascular Parkinson's disease and vascular dementia, is one of the most serious medical problems because it causes critical impairment of activity and quality of daily life. Regenerative medicine is now in the spotlight as a promising therapy to treat ischemic brain which has been considered to be irreversible and indicated for no active treatment. Various humoral factors are anticipated for their therapeutic potential for ischemic brain through neurogenic (*e.g.* basic fibroblast growth factor and epidermal growth factor) and angiogenic (*e.g.* vascular endothelial growth factor and hepatocyte growth factor) effects (43–47). Among them, we believe that the vascular hormone AM has several advantages as a therapeutic agent for ischemic brain. We can expect multiple effects of AM through its neuroprotective and vasculo-neuro-regenerative actions as shown in this study. In addition, AM has already been safely used for human patients with heart failure or pulmonary hypertension without any mention of critical adverse effects resulting from iv administration (39).

Thus, we are prompted to propose a new strategy to rescue ischemic brain by using vascular hormone AM for the combined neuroprotective and vasculo-neuro-regenerative therapy to improve impaired neurological function.

Acknowledgments

This work was supported by grants from Japanese ministry of Education, Culture, Sports, Science and Technology; ministry of Health, Labor and Welfare; and University of Kyoto 21st Century Centers of Excellence program. We thank Dr. Seiichi Hashida (Department of Biochemistry, University of Miyazaki) for measuring mature PAMP; and Dr. Kazuhiko Nozaki and Masaki Nishimura, (Department of Neurosurgery, University of Kyoto) for technical assistance.

Received August 15, 2005. Accepted December 19, 2005.

Address all correspondence and requests for reprints to: Hiroshi Itoh, M.D., Ph.D., Department of Medicine and Clinical Science, Kyoto University Graduate School of Medicine; 54 Shogoin Kawahara-cho, Sakyo-ku, Kyoto 606-8507, Japan. E-mail: hiito@kuhp.kyoto-u.ac.jp.

This work was supported by Japanese ministry of Education, Culture, Sports, Science and Technology; ministry of Health, Labor and Welfare; and University of Kyoto 21st Century Centers of Excellence program.

References

1. **Kitamura K, Kangawa K, Kawamoto M, Ichiki Y, Nakamura S, Matsuo H, Eto T** 1993 Adrenomedullin: a novel hypotensive peptide isolated from human pheochromocytoma. Biochem Biophys Res Commun 92:553–560
2. **Nagaya N, Mori H, Murakami S, Kangawa K, Kitamura S** 2005 Adrenomedullin: angiogenesis and gene therapy. Am J Physiol Regul Integr Comp Physiol 288:R1432–R1437
3. **Shindo T, Kurihara Y, Nishimatsu H, Moriyama N, Kakoki M, Wang Y, Imai Y, Ebihara A, Kuwaki T, Ju KH, Minamino N, Kangawa K, Ishikawa T, Fukuda M, Akimoto Y, Kawakami H, Imai T, Morita H, Yazaki Y, Nagai R, Hirata Y, Kurihara H** 2001 Vascular abnormalities and elevated blood pressure in mice lacking adrenomedullin gene. Circulation 104:1964–1971
4. **Shimosawa T, Shibagaki Y, Ishibashi K, Kitamura K, Kangawa K, Kato S, Ando K, Fujita T** 2002 Adrenomedullin, an endogenous peptide, counteracts cardiovascular damage. Circulation 105:106–111
5. **Imai Y, Shindo T, Maemura K, Sata M, Saito Y, Kurihara Y, Akishita M, Osuga J, Ishibashi S, Tobe K, Morita H, Oh-hashi Y, Suzuki T, Maekawa H, Kangawa K, Minamino N, Yazaki Y, Nagai R, Kurihara H** 2002 Resistance to neointimal hyperplasia and fatty streak formation in mice with adrenomedullin overexpression. Arterioscler Thromb Vasc Biol 22:1310–1315
6. **Miyashita K, Itoh H, Sawada N, Fukunaga Y, Sone M, Yamahara K, Yurugi-Kobayashi T, Park K, Nakao K** 2003 Adrenomedullin provokes endothelial Akt activation and promotes vascular regeneration both in vitro and in vivo. FEBS Lett 544:86–92
7. **Miyashita K, Itoh H, Sawada N, Fukunaga Y, Sone M, Yamahara K, Yurugi T, Nakao K** 2003 Adrenomedullin promotes proliferation and migration of cultured endothelial cells. Hypertens Res 26:S93–S98
8. **Abe M, Sata M, Nishimatsu H, Nagata D, Suzuki E, Terauchi Y, Kadowaki T, Minamino N, Kangawa K, Matsuo H, Hirata Y, Nagai R** 2003 Adrenomedullin augments collateral development in response to acute ischemia. Biochem Biophys Res Commun 306:10–15
9. **Kim W, Moon SO, Sung MJ, Kim SH, Lee S, So JN, Park SK** 2003 Angiogenic role of adrenomedullin through activation of Akt, mitogen-activated protein kinase, and focal adhesion kinase in endothelial cells. FASEB J 17:1937–1939
10. **Tokunaga N, Nagaya N, Shirai M, Tanaka E, Ishibashi-Ueda H, Harada-Shiba M, Kanda M, Ito T, Shimizu W, Tabata Y, Uematsu M, Nishigami K, Sano S, Kangawa K, Mori H** 2004 Adrenomedullin gene transfer induces therapeutic angiogenesis in a rabbit model of chronic hind limb ischemia: benefits of a novel nonviral vector, gelatin. Circulation 109:526–531
11. **Iwase T, Nagaya N, Fujii T, Itoh T, Ishibashi-Ueda H, Yamagishi M, Miyatake K, Matsumoto T, Kitamura S, Kangawa K** 2005 Adrenomedullin enhances angiogenic potency of bone marrow transplantation in a rat model of hindlimb ischemia. Circulation 111:356–362
12. **Eto T** 2001 A review of the biological properties and clinical implications of adrenomedullin and proadrenomedullin N-terminal 20 peptide (PAMP), hypotensive and vasodilating peptides. Peptides 22:1693–1711
13. **Serrano J, Alonso D, Fernandez AP, Encinas JM, Lopez JC, Castro-Blanco S, Fernandez-Vizarra P, Richart A, Santacana M, Uttenthal LO, Bentura ML, Martinez-Murillo R, Martinez A, Cuttitta F, Rodrigo J** 2002 Adrenomedullin in the central nervous system. Microsc Res Tech 57:76–90
14. **Wang X, Yue TL, Barone FC, White RF, Clark RK, Willette RN, Sulpizio AC, Aiyar NV, Ruffolo Jr RR, Feuerstein GZ** 1995 Discovery of adrenomedullin in rat ischemic cortex and evidence for its role in exacerbating focal brain ischemic damage. Proc Natl Acad Sci USA 92:11480–11484
15. **Dogan A, Suzuki Y, Koketsu N, Osuka K, Saito K, Takayasu M, Shibuya M, Yoshida J** 1997 Intravenous infusion of adrenomedullin and increase in regional cerebral blood flow and prevention of ischemic brain injury after middle cerebral artery occlusion in rats. J Cereb Blood Flow Metab 17:19–25
16. **Watanabe K, Takayasu M, Noda A, Hara M, Takagi T, Suzuki Y, Yoshia J** 2001 Adrenomedullin reduces ischemic brain injury after transient middle cerebral artery occlusion in rats. Acta Neurochir (Wien) 143:1157–1161
17. **Xia CF, Yin H, Borlongan CV, Chao J, Chao L** 2004 Adrenomedullin gene delivery protects against cerebral ischemic injury by promoting astrocyte migration and survival. Hum Gene Ther 15:1243–1254
18. **Hashida S, Kitamura K, Nagatomo Y, Shibata Y, Imamura T, Yamada K, Fujimoto S, Kato J, Morishita K, Eto T** 2004 Development of an ultrasensitive enzyme immunoassay for human proadrenomedullin N-terminal 20 peptide and direct measurement of two molecular forms of PAMP in plasma from healthy subjects and patients with cardiovascular disease. Clin Biochem 37:14–21
19. **Longa EZ, Weinstein PR, Carlson S, Cummins R** 1989 Reversible middle cerebral artery occlusion without craniectomy in rats. Stroke 20:84–91
20. **Teramoto T, Qiu J, Plumier JC, Moskowitz MA** 2003 EGF amplifies the replacement of parvalbumin-expressing striatal interneurons after ischemia. J Clin Invest 111:1125–1132
21. **Venditti A, Battaglia A, Del Poeta G, Buccisano F, Maurillo L, Tamburini A, Del Moro B, Epiceno AM, Martiradonna M, Caravita T, Santinelli S, Adorno G, Picardi A, Zinno F, Lanti A, Bruno A, Suppo G, Franchi A, Franconi G, Amadori S** 1999 Enumeration of CD34+ hematopoietic progenitor cells for clinical transplantation: comparison of three different methods. Bone Marrow Transplant 24:1019–1027
22. **Swanson RA, Morton MT, Tsao-Wu G, Savalos RA, Davidson C, Sharp FR** 1990 A semiautomated method for measuring brain infarct volume. J Cereb Blood Flow Metab 10:290–293
23. **Zhang ZG, Zhang L, Croll SD, Chopp M** 2002 Angiopoietin-1 reduces cerebral blood vessel leakage and ischemic lesion volume after focal cerebral embolic ischemia in mice. Neuroscience 2002 113:683–687

24. **Hayashi H, Ishisaki A, Imamura T** 2003 Smad mediates BMP-2-induced upregulation of FGF-evoked PC12 cell differentiation. FEBS Lett 536:30–34
25. **Iimuro S, Shindo T, Moriyama N, Amaki T, Niu P, Takeda N, Iwata H, Zhang Y, Ebihara A, Nagai R** 2004 Angiogenic effects of adrenomedullin in ischemia and tumor growth. Circ Res 95:415–423
26. **Nakano S, Kogure K, Fujikura H** 1990 Ischemia-induced slowly progressive neuronal damage in the rat brain. Neuroscience 38:115–124
27. **Graham SH, Chen J** 2001 Programmed cell death in cerebral ischemia. J Cereb Blood Flow Metab 21:99–109
28. **Northington FJ, Ferriero DM, Graham EM, Traystman RJ, Martin LJ** 2001 Early neurodegeneration after hypoxia-ischemia in neonatal rat is necrosis while delayed neuronal death is apoptosis. Neurobiol Dis 8:207–219
29. **Stoll G, Jander S, Schroeter M** 1998 Inflammation and glial responses in ischemic brain lesions. Prog Neurobiol 56:149–171
30. **Gilgun-Sherki Y, Rosenbaum Z, Melamed E, Offen D** 2002 Antioxidant therapy in acute central nervous system injury: current state. Pharmacol Rev 54:271–284
31. **Kim W, Moon SO, Lee S, Sung MJ, Kim SH, Park SK** 2003 Adrenomedullin reduces VEGF-induced endothelial adhesion molecules and adhesiveness through a phosphatidylinositol 3′-kinase pathway. Arterioscler Thromb Vasc Biol 23:1377–1383
32. **Kawai J, Ando K, Tojo A, Shimosawa T, Takahashi K, Onozato ML, Yamasaki M, Ogita T, Nakaoka T, Fujita T** 2004 Endogenous adrenomedullin protects against vascular response to injury in mice. Circulation 109:1147–1153
33. **Niu P, Shindo T, Iwata H, Iimuro S, Takeda N, Zhang Y, Ebihara A, Suematsu Y, Kangawa K, Hirata Y, Nagai R** 2004 Protective effects of endogenous adrenomedullin on cardiac hypertrophy, fibrosis, and renal damage. Circulation 109:1789–1794
34. **Krupinski J, Kaluza J, Kumar P, Kumar S, Wang JM** 1994 Role of angiogenesis in patients with cerebral ischemic stroke. Stroke 25:1794–1798
35. **Palmer TD, Willhoite AR, Gage FH** 2000 Vascular niche for adult hippocampal neurogenesis. J Comp Neurol 425:479–494
36. **Louissaint Jr A, Rao S, Leventhal C, Goldman SA** 2002 Coordinated interaction of neurogenesis and angiogenesis in the adult songbird brain. Neuron 34:945–960
37. **Asahara T, Murohara T, Sullivan A, Silver M, van der Zee R, Li T, Witzenbichler B, Schatteman G, Isner JM** 1997 Isolation of putative progenitor endothelial cells for angiogenesis. Science 275:964–967
38. **Taguchi A, Soma T, Tanaka H, Kanda T, Nishimura H, Yoshikawa H, Tsukamoto Y, Iso H, Fujimori Y, Stern DM, Naritomi H, Matsuyama T** 2004 Administration of CD34+ cells after stroke enhances neurogenesis via angiogenesis in a mouse model. J Clin Invest 114:330–338
39. **Nagaya N, Satoh T, Nishikimi T, Uematsu M, Furuichi S, Sakamaki F, Oya H, Kyotani S, Nakanishi N, Goto Y, Masuda Y, Miyatake K, Kangawa K** 2000 Hemodynamic, renal, and hormonal effects of adrenomedullin infusion in patients with congestive heart failure. Circulation 101:498–503
40. **Doi K, Itoh H, Ikeda T, Hosoda K, Ogawa Y, Igaki T, Yamashita J, Chun TH, Inoue M, Masatsugu K, Matsuda K, Ohmori K, Nakao K** 1997 Adenovirus-mediated gene transfer of C-type natriuretic peptide causes G1 growth inhibition of cultured vascular smooth muscle cells. Biochem Biophys Res Commun 239:889–894
41. **Komatsu Y, Itoh H, Suga S, Ogawa Y, Hama N, Kishimoto I, Nakagawa O, Igaki T, Doi K, Yoshimasa T, Nakao K** 1996 Regulation of endothelial production of C-type natriuretic peptide in coculture with vascular smooth muscle cells. Role of the vascular natriuretic peptide system in vascular growth inhibition. Circ Res 78:606–614
42. **Hippenstiel S, Witzenrath M, Schmeck B, Hocke A, Krisp M, Krull M, Seybold J, Seeger W, Rascher W, Schutte H, Suttorp N** 2002 Adrenomedullin reduces endothelial hyperpermeability. Circ Res 91:618–625
43. **Nakatomi H, Kuriu T, Okabe S, Yamamoto S, Hatano O, Kawahara N, Tamura A, Kirino T, Nakafuku M** 2002 Regeneration of hippocampal pyramidal neurons after ischemic brain injury by recruitment of endogenous neural progenitors. Cell 110:429–441
44. **Zhang ZG, Zhang L, Jiang Q, Zhang R, Davies K, Powers C, Bruggen N, Chopp M** 2000 VEGF enhances angiogenesis and promotes blood-brain barrier leakage in the ischemic brain. J Clin Invest 106:829–838
45. **Shimamura M, Sato N, Oshima K, Aoki M, Kurinami H, Waguri S, Uchiyama Y, Ogihara T, Kaneda Y, Morishita R** 2004 Novel therapeutic strategy to treat brain ischemia: overexpression of hepatocyte growth factor gene reduced ischemic injury without cerebral edema in rat model. Circulation 109:424–431
46. **Sun Y, Jin K, Xie L, Childs J, Mao XO, Logvinova A, Greenberg DA** 2003 VEGF-induced neuroprotection, neurogenesis, and angiogenesis after focal cerebral ischemia. J Clin Invest 111:1843–1851
47. **Sondell M, Lundborg G, Kanje M** 1999 Vascular endothelial growth factor has neurotrophic activity and stimulates axonal outgrowth, enhancing cell survival and Schwann cell proliferation in the peripheral nervous system. J Neurosci 19:5731–5740

Endocrinology **is published monthly by The Endocrine Society (http://www.endo-society.org), the foremost professional society serving the endocrine community.**

0021-972X/07/$15.00/0
Printed in U.S.A.

The Journal of Clinical Endocrinology & Metabolism 92(3):1066–1072

doi: 10.1210/jc.2006-1621

Antithyroid Drugs Inhibit Thyroid Hormone Receptor-Mediated Transcription

Kenji Moriyama, Tetsuya Tagami, Takeshi Usui, Mitsuhide Naruse, Takuo Nambu, Yuji Hataya, Naotetsu Kanamoto, Yu-shu Li, Akihiro Yasoda, Hiroshi Arai, and Kazuwa Nakao

Department of Medicine and Clinical Science (K.M., T.N., Y.H., N.K., Y.L., A.Y., H.A., K.N.), Graduate School of Medicine, Kyoto University, Kyoto 606-8507, Japan; and Division of Endocrinology and Metabolism (K.M., T.T., T.U., M.N.), Clinical Research Institute, Kyoto Medical Center, National Hospital Organization, Kyoto 612-8555, Japan

Context: Methimazole (MMI) and propylthiouracil (PTU) are widely used as antithyroid drugs (ATDs) for the treatment of Graves' disease. Both MMI and PTU reduce thyroid hormone levels by several mechanisms, including inhibition of thyroid hormone synthesis and secretion. In addition, PTU decreases 5′-deiodination of T_4 in peripheral tissues. ATDs may also interfere with T_3 binding to nuclear thyroid hormone receptors (TRs). However, the effect of ATDs on the transcriptional activities of T_3 mediated by TRs has not been studied.

Objective: The present study was undertaken to determine whether ATDs have an effect on the gene transcription regulated by T_3 and TRs *in vitro*.

Methods: Transient gene expression experiments and GH secretion assays were performed. To elucidate possible mechanisms of the antagonistic action of ATDs, the interaction between TR and nuclear cofactors was examined.

Results: In the transient gene expression experiments, both MMI and PTU significantly suppressed transcriptional activities mediated by the TR and T_3 in a dose-dependent manner. In mammalian two-hybrid assays, both drugs recruited one of the nuclear corepressors, nuclear receptor corepressor, to the TR in the absence of T_3. In addition, PTU dissociated nuclear coactivators, such as steroid receptor coactivator-1 and glucocorticoid receptor interacting protein-1, from the TR in the presence of T_3. Finally, MMI decreased the GH release that was stimulated by T_3.

Conclusions: ATDs inhibit T_3 action by recruitment of transcriptional corepressors and/or dissociation of coactivators. This is the first report to show that ATDs can modulate T_3 action at the transcriptional level. (***J Clin Endocrinol Metab* 92: 1066–1072, 2007**)

THYROID HORMONES REGULATE growth, development, and critical metabolic functions. They exert these effects through complex biological pathways, which offer a wealth of opportunity to intervene pharmacologically in thyroid hormone signaling at numerous steps. These include biosynthesis, cell-specific uptake, or export of thyroid hormone as well as nuclear targeting and actions, which are exerted through thyroid hormone receptor (TR) binding and histone acetylation. Such processes represent potentially important pharmacological targets for the drug therapies of thyroid hormone abnormalities, especially hyperthyroidism.

Some compounds having thionamide structure, such as thiourea and thiouracil, inhibit thyroid function. Clinically used antithyroid drugs (ATDs) include methimazole (1-methyl-2-mercaptoimidazole; MMI), and propylthiouracil (6-propyl-2-thiouracil; PTU) to treat Graves' hyperthyroidism (Fig. 1). ATDs have intrathyroidal and extrathyroidal actions. The chief intrathyroidal actions include inhibition of iodine oxidation and organization and iodotyrosine coupling, among others. The main extrathyroidal action is inhibition of conversion of T_4 to T_3 by PTU, but not MMI (1, 2). Thus, the reduction in thyroid hormone production induced by the drugs is central to these actions.

Furthermore, ATDs are known to influence oxygen consumption, or peripheral metabolic suppression, although the mechanisms are not fully understood (3, 4). To date, a number of studies was performed to elucidate how ATDs suppress peripheral metabolism. ATDs can affect gene expression and modulate functions of some cell types (5). Although ATDs were not effective in the binding affinity of T_4 to serum thyroxine binding globulin, they inhibited T_3 binding to the hepatic nuclear extracts (6). However, the effect of ATDs on the transcriptional activities of T_3 mediated by TRs has not been studied in detail. The present study was undertaken to determine whether ATDs have an effect on the gene transcription regulated by T_3 and TRs *in vitro*.

Materials and Methods

Reagents

The chemical structures of PTU, MMI, and T_3 are shown in Fig. 1. ATDs were purchased from Sigma-Aldrich, Corp. (St. Louis, MO). T_3 was purchased from Nakalai Tesque Inc. (Kyoto, Japan).

Plasmid constructions

Expression vectors containing wild-type human TRβ1 (pCMX-hTRβ1) and human TRα1 (pCMX-hTRα1) were provided by K. Ume-

First Published Online December 27, 2006

Abbreviations: AF, Activation function; ATD, antithyroid drug; CoA, coactivator protein; CoR, corepressor protein; DBD, DNA binding domain; FBS, fetal bovine serum; GRIP, glucocorticoid receptor interacting protein; LBD, ligand-binding domain; Luc, luciferase; MMI, methimazole; NCoR, nuclear receptor corepressor; PTU, propylthiouracil; SMRT, silencing mediator of retinoid and thyroid receptor; SRC, steroid receptor coactivator; TK, thymidine kinase; TR, thyroid hormone receptor; TRE, thyroid hormone response element.

A Triiodothyronine (T3)

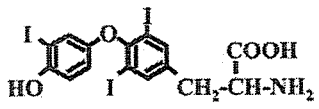

B Propylthiouracil (PTU)

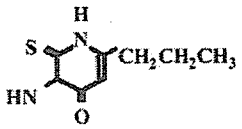

C Methimazole (MMI)

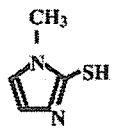

FIG. 1. The structure of T_3 and two antithyroid drugs, propylthiouracil and methimazole.

sono (Salk Institute, San Diego, CA) (7). The ligand-binding domain (LBD) of TRα1 or TRβ1 was fused to the DNA binding domain (DBD) of Gal4 in-frame in pSG424 (8). The Gal4-NCoR (residues 1552–2453), Gal4-SRC1 (residues 213-1061), and Gal4-GRIP1 (residues 480-1462) constructs contain the indicated TR interaction domains of these proteins (9). The VP16 construct for TRβ contains the LBD of the receptor downstream of the VP16 activation domain in-frame in pCMX (9). The reporter plasmids, TRE-TK-Luc (9) and ME-TK-Luc (10), contain two copies of a palindromic thyroid hormone response elements (TRE) and malic enzyme, respectively, upstream of the thymidine kinase (TK) promoter in the pA3-luciferase vector (Luc). TSHα-Luc contains 846 bp of the 5′-flanking sequence and 44 bp of exon I from the human glycoprotein hormone α-subunit gene in pA3-Luc (9). The Gal4 reporter plasmid, UAS-E1BTATA-Luc, contains five copies of the Gal4 recognition sequence (UAS) upstream of E1BTATA in pA3-Luc (11). The pRL-TK vector (Promega Corp., Madison, WI) comprised of the tk promoter and *Renilla* luciferase cDNA was used as an internal control.

Cell culture

TSA201, a clone of human embryonic kidney 293 cells (12), human hepatoblastoma HepG2 cells, and rat pituitary GH3 cells were maintained in DMEM, containing penicillin (100 U/ml) and streptomycin (100 μg/ml) with 10% fetal bovine serum (FBS; Invitrogen, Corp., Carlsbad, CA). For hormone and drug treatment, the medium was changed to phenol red-free DMEM (Nikken Biomedical Laboratory, Kyoto, Japan) containing 10% charcoal-stripped FBS (13).

Transient expression assays

TSA201 and HepG2 cells were grown in phenol red-free DMEM (Nikken Biomedical Laboratory) with 10% charcoal-stripped FBS and were transfected using the calcium precipitation method (14). After exposure to the calcium phosphate-DNA precipitate for 8 h, phenol red-free DMEM with charcoal-stripped FBS was added, in the absence or presence of compounds and/or T_3. Cells were harvested for measurements of luciferase activity, according to the manufacturer's instructions (dual-luciferase reporter assay system; Promega). The transfection efficiencies were corrected with the internal control. Both firefly and *Renilla* luciferase activities were measured to monitor the transfection efficiency and cytotoxicity of the added materials. The firefly activity obtained by the T_3-specific promoter was divided by the *Renilla* activity obtained by the nonspecific promoter in each well. Results are expressed as the mean ± SD from at least three transfections, each performed in triplicate. Data were analyzed by ANOVA with *post hoc* Dunnett's tests to compare with the control.

GH secretion and assay

For GH assays, GH3 cells, derived from the rat pituitary tumor cell line, were seeded into 6-well plates at 1.5×10^4 cells/well. T_3 (1 nM) as a physiological concentration and/or 10 μM MMI was added on the day after the medium was replaced. In the case of 10 μM PTU, cell survival was inhibited and the assay was abandoned. Culture media were collected after 2 d of incubation and GH was measured by ELISA (rat GH enzyme-immunoassay system; GE Healthcare UK Ltd., Buckinghamshire, UK) according to the manufacturer's instructions. After harvesting the supernatant, cell numbers were counted to evaluate cell proliferation. Results are expressed as the mean ± SD from at least five experiments, each performed in quadricate. Data were analyzed by ANOVA with *post hoc* Dunnett's tests to compare with the control.

Results

ATDs suppressed transcriptional activities mediated by TRα1 and TRβ1

The chemical structure of T_3, PTU, and MMI are shown in Fig. 1. ATDs are known as thionamides, which contain a sulfhydryl group and a thiourea moiety within a heterocyclic structure. Takagi *et al.* (6) reported that ATDs inhibit specific binding of T_3 to its receptor, perhaps due to an interaction with cysteine residues of the receptor.

We examined whether ATDs antagonize T_3-induced TR activation. Transient expression experiments were performed using TSA201 cells, which are a derivative of human embryonic kidney 293 cells. The LBD of TRα1 or TRβ was fused to the DNA binding domain of the yeast transcription factor, Gal4, and was cotransfected with a Gal4 reporter gene, UAS-E1BTATA-Luc. We determined the effects of ATDs on various physiological concentrations of T_3. In the presence of 10 μM PTU, increasing amounts of T_3 were added to the medium, and transcriptional activity was measured. PTU had no significant effects on TR-mediated transcriptional activity in the absence of T3 (Fig. 2) and in the absence of Gal4-TR (see Fig. 6A). However, PTU suppressed the activity mediated by Gal4-TRα1 up to 36% and Gal4-TRβ up to 39% of the respective control levels in the presence of T_3. The maximum suppression by PTU was obtained at the concentration of 1 nM of T_3. Similar results were obtained using MMI (data not shown).

The inhibitory effects of ATDs were also examined in the context of native receptors. A T_3-responsive reporter gene, TRE-TK-Luc, was cotransfected with full-length TRs (Fig. 3A). ATDs did not affect the activity of TRE-TK-Luc alone without TR. In the presence of 1 nM T_3, dose-dependent inhibition of transcription mediated by TRα1 and TRβ1 was observed with both ATDs. PTU suppressed the TRα1-mediated activity by 45% and TRβ1-mediated activity by 39% and MMI suppressed TRα1-mediated activity by 45% and TRβ1-mediated activity by 53% of the respective T_3 effect.

In a reciprocal manner, another group of negatively regulated genes was stimulated by TRs in the absence of T_3 and was repressed in response to T_3 (14). The effects of ATDs on the TSHα promoter were examined as a model of a negatively regulated gene. As shown in Fig. 3B, although PTU did

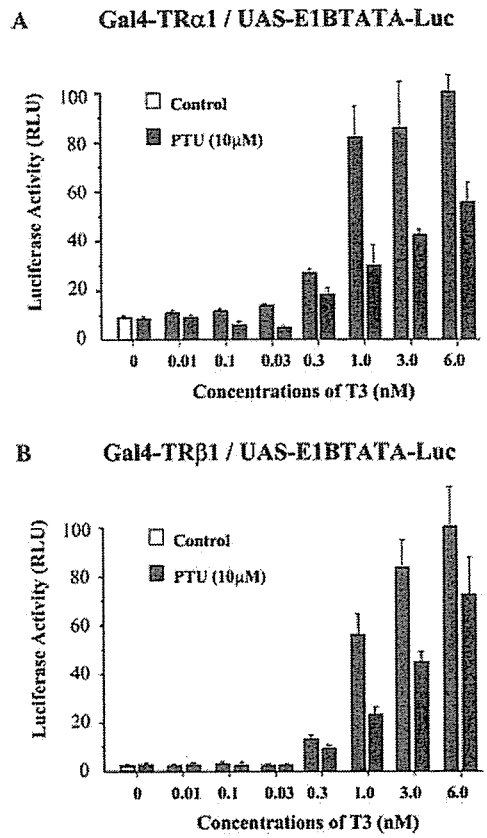

FIG. 2. ATDs suppress TR-mediated transcription in the presence of a physiological range of T_3. Gal4-TRα1 (A) or Gal4-TRβ1 (B; 50 ng) was cotransfected into TSA-201 cells with 100 ng of the reporter gene, UAS-E1BTATA-Luc, in the absence or presence of 10 μM PTU. RLU, Relative light units. The firefly activity obtained by UAS-E1BTATA-Luc was normalized to the *Renilla* activity obtained by PRL-TK-Luc.

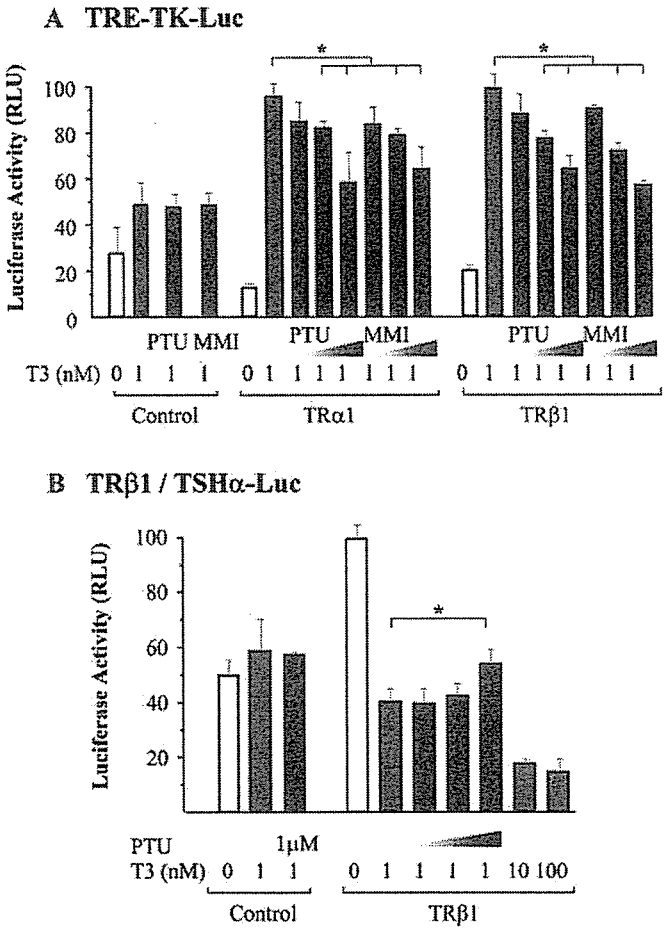

FIG. 3. The inhibitory effects of ATDs on the gene transcription mediated by native TR. A, The CMX, CMX-TRα1, or CMX-TRβ1 (50 ng) was cotransfected into TSA-201 cells with 100 ng of the reporter gene, TRE-TK-Luc, in the absence or presence of 1 nM T_3 and increasing amount of ATDs. B, The CMX or CMX-TRβ1 (50 ng) was cotransfected into TSA-201 cells with 100 ng of the reporter gene, TSHα-Luc, in the absence or the presence of 1 nM T_3 and increasing amount of PTU (1 nM, 100 nM, and 10 μM). RLU, Relative light units. The firefly activity obtained by TRE-TK-Luc or TSHα-Luc was normalized to the *Renilla* activity obtained by PRL-TK-Luc. *, $P < 0.05$.

not affect the activity of TSHα-Luc alone without TR, PTU increased the transcriptional activity, which was suppressed by 1 nM T_3 up to the control level. Similar results were obtained using MMI (data not shown).

The inhibitory effects of PTU were also examined at high concentrations of T_3. In the presence of 100 nM of T_3, which is almost 20 times greater than concentrations found in blood samples of patients with severe hyperthyroidism, the effects of PTU were eliminated (Fig. 4). Similar results were obtained using MMI (data not shown).

ATDs suppressed transcriptional activities mediated by endogenous TRs

We next studied the effects of ATDs using a cell line that contains physiological amounts of endogenous TRs. The reporter gene regulated by the ME-TRE, ME-TK-Luc, was transfected into human hepatoblastoma, HepG2. No significant effects were observed by 48 h incubation with 10 μM PTU or MMI on the ME-TK-Luc activity in the absence of T_3. One nanomole T_3 stimulated the activity by 1.8-fold, compared with that without T_3, and ATDs inhibited its increase by 70% (Fig. 5).

ATDs recruit corepressor and dissociate coactivator

Transcriptional repression of the positively regulated genes by unliganded TR is mediated by interacting with corepressor proteins (CoRs) such as nuclear receptor corepressor (NCoR) (15) and silencing mediator of retinoid and thyroid receptors (SMRT) (16). CoRs might also be involved in the basal activation of negatively regulated genes (14). In the other hand, in the presence of T_3, liganded TR activates transcription of the positively regulated genes and inhibits that of the negatively regulated genes by interacting with coactivator proteins (CoAs) (17) such as steroid receptor coactivator (SRC)-1 (18) and glucocorticoid-interacting protein (GRIP)-1 (19). Using a mammalian two-hybrid assay, the effect of ATDs on the TR-CoR or TR-CoA interaction was examined. The TR interaction domain of CoRs or CoAs was fused to the Gal4-DBD. The LBD of TRβ was fused to the transcriptional activation domain of VP16 to allow detection of the interaction between the Gal4-CoR/CoA and VP16-TR.

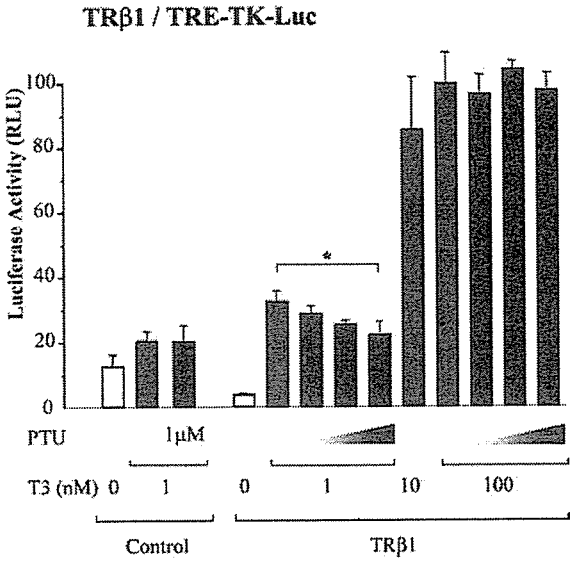

FIG. 4. High amount of T_3 blocks the inhibitory effects of ATDs on the gene transcription mediated by native TR. The CMX or CMX-TRβ1 (50 ng) was cotransfected into TSA-201 cells with 100 ng of the reporter gene, TRE-TK-Luc, in the absence or the presence of 1 or 100 nM T_3 and an increasing amount of PTU (1 nM, 100 nM, and 10 μM). RLU, Relative light units. The firefly activity obtained by TRE-TK-Luc was normalized to the *Renilla* activity obtained by PRL-TK-Luc. *, $P < 0.05$.

As shown in Fig. 6A, both PTU and MMI had no significant effects on the activity mediated by Gal4-DBD and VP16-TR. PTU enhanced TR-NCoR interaction but not TR-SMRT interaction in a dose-dependent manner (Fig. 6B). In contrast, PTU inhibited TR-SRC1 interaction and, to a lesser degree, TR-GRIP1 interaction in a dose-dependent manner (Fig. 6D). Similarly, MMI enhanced TR-NCoR interaction but not TR-SMRT interaction and inhibited TR-GRIP1 interaction but not TR-SRC1 interaction (Fig. 6, C and E).

ATDs inhibited endogenous hormone secretion induced by T_3

T_3 stimulates endogenous GH gene transcription mediated by endogenous TRs in rat pituitary tumor cells (20–22).

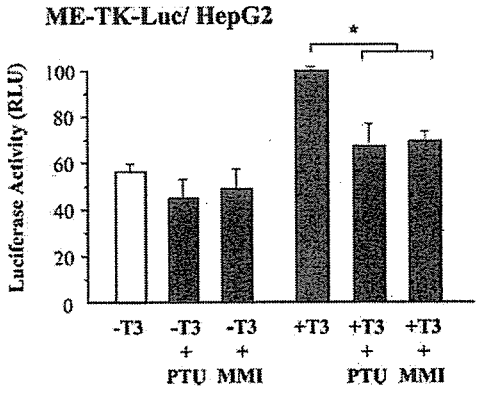

FIG. 5. ATDs suppress transcriptional activities mediated by endogenous TRs. The ME-TK-Luc (100 ng) was transfected into HepG2 cells and incubated with or without 1 nM T_3 and/or 10 μM PTU or MMI for 48 h. RLU, Relative light units. The firefly activity obtained by ME-TK-Luc was normalized to the *Renilla* activity obtained by PRL-TK-Luc. *, $P < 0.05$.

The production of GH was measured by ELISA in the culture media of GH3 cells. Forty-eight-hour incubation with 1 nM T_3 stimulated the GH production by 2.7-fold (Fig. 7). Addition of 10 μM MMI significantly decreased the GH release to 82% of that with 1 nM T_3 alone. In the case of 10 μM PTU, cell death was induced (data not shown).

Discussion

The ATDs have been a mainstay of treatment of patients with Graves' hyperthyroidism (23). The ATDs are heterocyclic compounds known as thionamides that contain a thioureylene group (Fig. 1). Two kinds of drugs of this type are available at present: one is MMI and carbimazole (1-methyl-2-thio-3-carbethxy-imidazole), which is rapidly metabolized to MMI, and the other is PTU. These drugs cause goiter in animals, which is due to the stimulation of the thyroid by the pituitary, consequent to pharmacological inhibition of thyroid hormone production (24, 25). Thus, derivatives of thiourea and thiouracil have been used as antithyroid drugs for more than 60 yr.

The main effect of ATDs is to inhibit the synthesis of T_4 and T_3 as an intrathyroidal action, including inhibition of iodine oxidation and organization, inhibition of iodotyrosine coupling, possible alteration of thyroglobulin structure, and inhibition of thyroglobulin biosynthesis. As an extrathyroidal action, PTU but not MMI inhibits conversion of T_4 to T_3. During the last 3 decades, reports have been accumulating on extrathyroidal actions of the ATDs, especially of the thionamide group, causing several undesirable side effects. Bandyopadhyay *et al.* (5) reviewed extrathyroidal actions of antithyroid thionamides in animals and humans. Thionamides inhibit lactoperoxidase, which contributes to the antibacterial activities of a number of mammalian exocrine gland secretions that protect a variety of mucosal surfaces. These drugs stimulate both gastric acid and pepsinogen secretions, thereby augmenting the severity of gastric ulcers and preventing wound healing. Severe abnormalities may develop in blood cells and the immune system after thionamide therapy. They may cause agranulocytosis, aplastic anemia, and purpura along with immune suppression. Olfactory and auditory systems are also affected by these drugs. Thionamide affects the sense of smell and taste and may also cause loss of hearing. Thionamide also affects gene expression and modulate the functions of some cell types.

After administration of ATDs to patients with Graves' disease, it usually takes 2 or 3 d to start decreasing serum level of T_4 and T_3. However, O_2 consumption or other peripheral metabolic indexes indicated that ATDs exerted an immediate effect *in vivo* (4, 5). Besides a specific effect of PTU as a 5′-deiodinase inhibitor effectively preventing T_3 generation, those actions were reported to persist in the presence of both of ATDs. Because thyroid hormones directly activate the expression of the human and mouse uncoupling protein-3 genes through a thyroid response element in the proximal promoter region, peripheral metabolism was controlled most partly by thyroid hormone level (26). An immediate effect of both of ATDs might be involved in the inhibition of transcriptional activities by thyroid hormone.

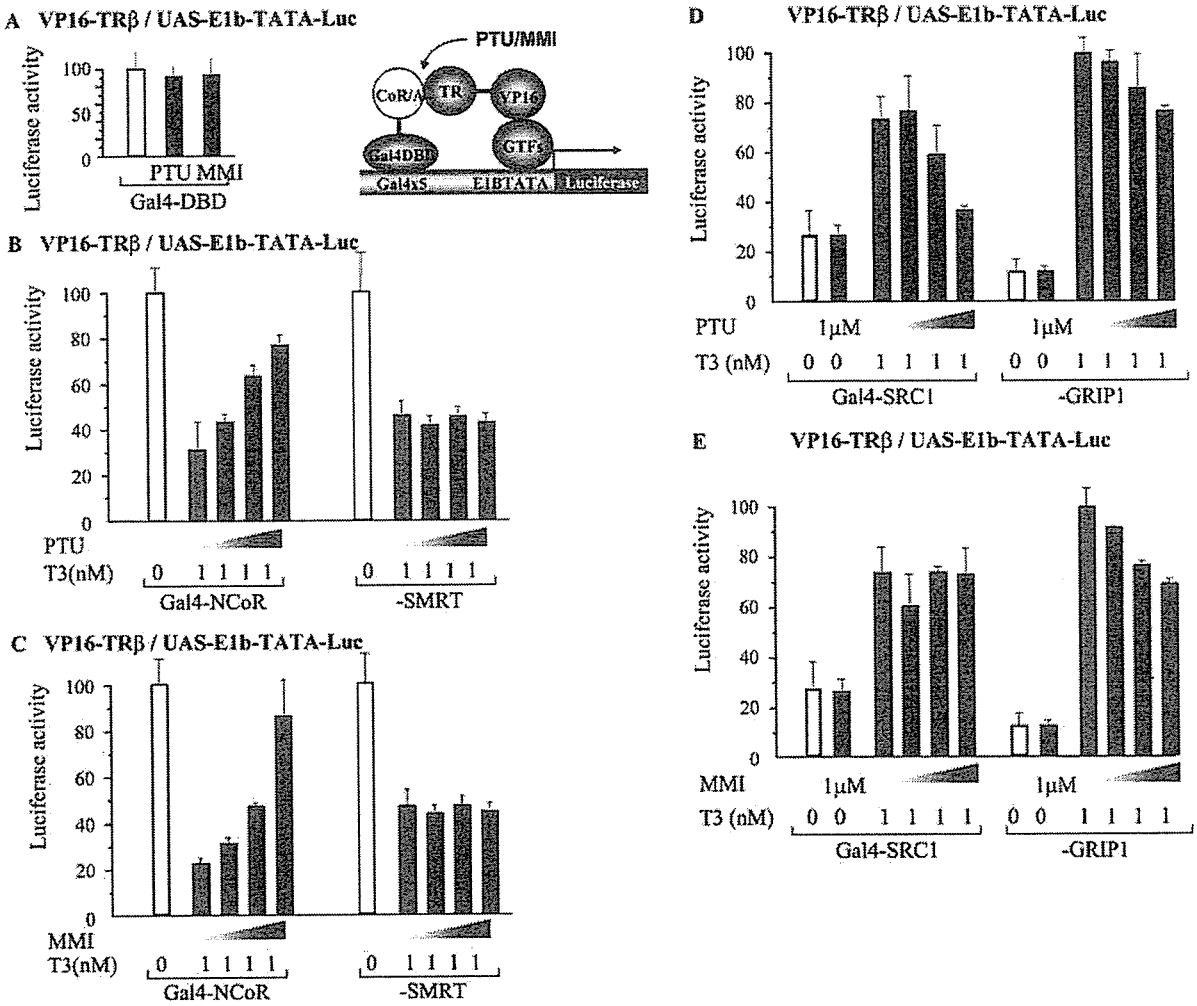

FIG. 6. The effects of ATDs on the interaction between TR and cofactors. The format of the mammalian two-hybrid experiment is shown *between panels A and D*. Gal4 fusion plasmids of indicated cofactors (50 ng) were cotransfected into TSA-201 cells with 100 ng of VP16-TRβ together with 100 ng of the reporter gene, UAS-E1BTATA-Luc, in the absence or presence of 1 nM T3. Increasing amounts (1 nM, 100 nM, and 10 μM) of PTU or MMI were added. A, Gal4-DBD. B and C, Gal4-NCoR and Gal4-SMRT. D and E, Gal4-SRC1 and Gal4-GRIP1. RLU, Relative light units. The firefly activity obtained by UAS-E1BTATA-Luc was normalized to the *Renilla* activity obtained by PRL-TK-Luc. GTF, General transcription factor.

Induction of cell proliferation by mitogen or growth factor stimulation leads to the specific and sequential expression of a large number of genes. To date several reports showed that ATDs change mRNA expression level of certain genes. MMI and PTU increase thyroglobulin gene expression and increase thyroid-specific mRNA concentration in human thyroid FRTL-5 cells (27–29). The stimulatory effects of MMI and PTU can be suppressed by iodide and do not occur when protein synthesis is inhibited by cycloheximide. MMI and PTU increased thyroid peroxidase mRNA in cultured porcine thyroid follicles (30). MMI can suppress the interferon-γ-induced increase in HLA-DRα gene expression (31). Fas ligand expression is induced by MMI in follicular cells of thyroid glands obtained from Graves' patients and cultured thyrocytes, resulting in Fas ligand-dependent apoptosis of thyrocytes (32). In the thyroid, the TR expression has been reported (33–35).

ATDs are mainly concentrated in the thyroid gland but more than 70% of ATDs are unevenly distributed in the whole body (36). Therefore, the transcriptional inhibition by ATDs in the periphery may be dependent on the concentration of ATDs in each tissue. The peak serum concentrations of MMI are in the range of 300 ng/ml (2.6 mM) after a 15-mg oral dose (37), and those of PTU are about 3 mg/ml (18 mM) after a 150-mg oral dose (38). As we have shown here, inhibition of T_3 action was observed for GH expression (20–22) in rat pituitary GH3 cells and for malic enzyme expression (10) in human hepatic HepG2 cells. However, the inhibitory effects on cell proliferation of these cells were also seen under the therapeutic concentrations of ATDs.

Takagi *et al.* (6) demonstrated that thionamides inhibit specific T_3 binding to the hepatic nuclear receptor. MMI and PTU at a pharmacological dose (2 mM) reduced specific T_3 binding to chromatographed nuclear receptors by 84 and 85%, respectively. Scatchard analyses indicated that neither MMI nor PTU significantly altered the affinity constant, whereas they both

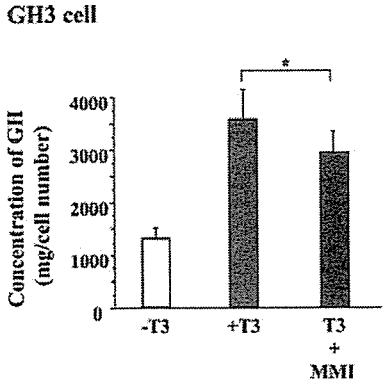

FIG. 7. The inhibitory effects of ATDs on the GH secretion induced by T_3. GH3 cells were incubated with or without 1 nM T_3 and/or 10 μM MMI for 48 h. Culture media were collected and GH was measured by ELISA. *, $P < 0.05$.

decreased maximal binding capacity. We obtained similar results using rat liver nuclear extract (data not shown) (13). Thereafter, there is no study of the actions of ATDs on the transcriptional regulation mediated by T_3 and TR.

In this study we demonstrated that ATDs could impair thyroid hormone action by suppressing its transcriptional activity. Gene suppression is attributed partly to the recruitment of NCoR and dissociation of GRIP1 or SRC1. In the case of positively regulated promoter, TRE-TK, the effect of T_3 was supposed to be inhibited by recruiting NCoR and dissociating GRIP1 or SRC1 by ATDs. In contrast, in the negatively regulated promoter, TSHα, the opposite effect was observed because corepressors may be involved in basal stimulation in the absence of T_3 (14) and coactivators may be involved in T_3-dependent inhibition in the presence of T_3 (17). A number of nuclear cofactors have been cloned, but most of their specific functions are unclear (39). These cofactors were initially studied in the context of the TR and other nuclear hormone receptors. However, every cofactor has multiple interaction domains comprised of subtly distinct LXXLL motif and its combination and seems to interact with multiple receptors in a different way. Each specific ligand also contributes conformational change of the receptor and modulates the cofactor binding to the receptor as an agonist or an antagonist. Indeed, PTU and MMI enhanced recruitment of NCoR but not SMRT to the TR and both drugs dissociated GRIP1, but dissociation of SRC1 occurred solely by PTU. NCoR preferentially bind TR homodimer over TR-RXR heterodimer (40) and TR prefers to recruit NCoR, and retinoid acid receptor prefers to recruit SMRT (41). These preferences are likely due to sequence differences in interacting domains of corepressors (42).

Conformational change of TR induced by ATDs may be subtly different from that induced by T_3, and it may enhance the interaction with specific domain of NCoR. The functional specificity is also reported among SRC family members. For example, progesterone receptor interacts preferentially with SRC1, which recruits cAMP response element-binding protein (CREB) binding protein (CBP) and enhances acetylation of histone H4, whereas glucocorticoid receptor interacts preferentially with SRC2 (GRIP1), which recruits p300/CBP-associated factor and results in histone H3 acetylation (43). PTU and MMI may have some different effect on the interaction between TR and SRC family members via their subtly distinct LXXLL motifs. Every receptor also has more than one activation domain [activation function (AF)-1 and AF-2]. Coactivators may preferentially use specific activation domains, depending on the receptor or activation function (AF-1 *vs.* AF-2) that is mediating the response to hormone (44). AF2 is conserved among nuclear hormone receptor superfamily as ligand-inducible transcription factors (45). We also tested the effects of ATDs on transcription mediated by other nuclear hormone receptors such as estrogen receptor-α and -β. ATDs had no effects on estrogen action (data not shown).

In summary, our findings demonstrate that ATDs, which are the most prevalent drugs to treat Graves' diseases, suppress transcriptional activity by modulating the cofactor recruitment to the TR. Although the clinical and therapeutic significance of our findings remains to be established, our data provide a mechanistic basis for one of the extrathyroidal actions of ATDs. It might be helpful in designing new therapeutic compounds with modifications of existing ATDs to enhance transcriptional inhibition against T_3 action.

Acknowledgments

The authors thank Ms. K. Matsuda, Ms. M. Kouchi, and Ms. H. Hiratani for their excellent secretarial assistance and Dr. S. Sasaki for technical assistance. We are also grateful to Dr. J. Larry Jameson for comments and suggestions on the manuscript.

Received July 27, 2006. Accepted December 14, 2006.

Address all correspondence and requests for reprints to: Tetsuya Tagami, M.D., Ph.D., Division of Endocrinology and Metabolism, Clinical Research Institute, Kyoto Medical Center, National Hospital Organization, Kyoto 612-8555, Japan. E-mail: ttagami@kyotolan.hosp.go.jp.

This work was supported in part by the grants from The Smoking Research Foundation (to K.M.) and The Japanese Ministry of Education and Science (11671103 and 17590973; to T.T.).

Disclosure Statement: The authors have nothing to disclose.

References

1. **Cooper DS** 1984 Antithyroid drugs. N Engl J Med 311:1353–1362
2. **Cooper DS** 2005 Antithyroid drugs. N Engl J Med 352:905–917
3. **Meredish JH, Rogers H, Johnston FR** 1961 Immediate influence of propylthiouracil on oxygen consumption in the dog. Surg Forum 12:5–7
4. **Bray GA, Hildreth S** 1967 Effect of propylthiouracil and methimazole on the oxygen consumption of hypothyroid rats receiving thyroxine or triiodothyronine. Endocrinology 81:1018–1020
5. **Bandyopadhyay U, Biswas K, Banerjee RK** 2002 Extrathyroidal actions of antithyroid thionamides. Toxicol Lett 128:117–127
6. **Takagi S, Hummel BC, Walfish PG** 1990 Thionamides and arsenite inhibit specific T_3 binding to the hepatic nuclear receptor. Biochem Cell Biol 68:616–621
7. **Umesono K, Murakami KK, Thompson CC, Evans RM** 1990 Direct repeats as selective response elements for the thyroid hormone, retinoic acid, and vitamin D receptors. Cell 65:1255–1266
8. **Sadowski I, Ma J, Tiezenberg S, Ptashne M** 1988 Gal4-VP16 is an unusually potent transcriptional activator. Nature 335:563–564
9. **Tagami T, Gu W, Peairs PT, West BL, Jameson JL** 1998 A novel natural mutation in the thyroid hormone receptor defines a dual functional domain that exchanges nuclear receptor corepressors and coactivators. Mol Endocrinol 12:1888–1902
10. **Desvergne B, Petty KJ, Nikodem VM** 1991 Functional characterization and receptor binding studies of the malic enzyme thyroid hormone response element. J Biol Chem 266:1008–1013
11. **Tagami T, Lutz WH, Kumar R, Jameson JL** 1998 The interaction of the vitamin D receptor with nuclear receptor corepressors and coactivators. Biochem Biophys Res Commun 253:353–363
12. **Margolskee RF, McHendry-Rinde B, Horn R** 1993 Panning transfected cells for electrophysiological studies. Biotechniques 15:906–911
13. **Moriyama K, Tagami T, Akamizu T, Usui T, Saijo M, Kanamoto N, Hataya**

Y, Simatsu A, Kuzuya H, Nakao K 2002 Thyroid hormone action is disrupted by Bisphenol A as an antagonist. J Clin Endocrinol Metab 87:5185–5190
14. Tagami T, Madison LD, Nagaya T, Jameson JL 1997 Nuclear receptor corepressors activate rather than suppress basal transcription of genes that are negatively regulated by thyroid hormone. Mol Cell Biol 17:2642–2648
15. Horlein AJ, Naar AM, Heinzel T, Torchia J, Gloss B, Kurokawa R, Ryan A, Kamei Y, Soderstrom M, Glass CK, Rosenfeld MG 1995 Ligand-independent repression by the thyroid hormone receptor mediated by a nuclear receptor co-repressor. Nature 377:397–404
16. Chen JD, Evans RM 1995 A transcriptional co-repressor that interacts with nuclear hormone receptors. Nature 377:454–457
17. Tagami T, Park Y, Jameson JL 1999 Mechanisms that mediate negative regulation of the thyroid stimulating hormone gene by the thyroid hormone receptor. J Biol Chem 274:22345–22353
18. Onate SA, Tsai SY, Tsai MJ, O'Malley BW 1995 Sequence and characterization of a coactivator for the steroid hormone receptor superfamily. Science 270: 1354–1357
19. Hong H, Kohli K, Garabedian MJ, Stallcup MR 1997 GRIP1, a transcriptional coactivator for the AF-2 transactivation domain of steroid, thyroid, retinoid, and vitamin D receptors. Mol Cell Biol 17:2735–2744
20. Glass CK, Franco R, Weinberger C, Albert VR, Evans RM, Rosenfeld MG 1987 A c-erb-A binding site in rat growth hormone gene mediates transactivation by thyroid hormone. Nature 329:738–741
21. Koenig RJ, Brent GA, Warne RL, Larsen PR, Moore DD 1987 Thyroid hormone receptor binds to a site in the rat growth hormone promoter required for induction by thyroid hormone. Proc Natl Acad Sci USA 84:5670–5674
22. Koenig RJ, Warne RL, Brent GA, Harney JW, Larsen PR, Moore DD 1988 Isolation of a cDNA clone encoding a biologically active thyroid hormone receptor. Proc Natl Acad Sci USA 85:5031–5035
23. Astwood EB 1943 Treatment of hyperthyroidism with thiourea and thiouracil. JAMA 122:78
24. Mackinzie JB, Mackinzie CG, McCollum EV 1941 The effect of sulfanilylguanidine on the thyroid of the rat. Science 94:518
25. Mackinzie CG, Mackinzie JB 1943 The effect of sulfonamides and thiouracil on the thyroid gland and basal metabolism. Endocrinology 32:185
26. Solanes G, Pedraza N, Calvo V, Vidal-Puig A, Lowell BB, Villarroya F 2005 Thyroid hormones directly activate the expression of the human and mouse uncoupling protein-3 genes through a thyroid response element in the proximal promoter region. Biochem J 386:505–513
27. Leer LM, Cammenga M, van der Vorm ER, de Vijlder JJ 1991 Methimazole increases thyroid-specific mRNA concentration in human thyroid cells and FRTL-5 cells. Mol Cell Endocrinol 78:221–228
28. Leer LM, Cammenga M, de Vijlder JJ 1991 Methimazole and propylthiouracil increase thyroglobulin gene expression in FRTL-5 cells. Mol Cell Endocrinol 82:R25–R30
29. Isozaki O, Tsushima T, Emoto N, Saji M, Tsuchiya Y, Demura H, Sato Y, Shizume K, Kimura S, Kohn LD 1991 Methimazole regulation of thyroglobulin biosynthesis and gene transcription in rat FRTL-5 thyroid cells. Endocrinology 128:3113–3121
30. Sugawara M, Sugawara Y, Wen K 1999 Methimazole and propylthiouracil increase cellular thyroid peroxidase activity and thyroid peroxidase mRNA in cultured porcine thyroid follicles. Thyroid 9:513–518
31. Montani V, Shong M, Taniguchi SI, Suzuki K, Giuliani C, Napolitano G, Saito J, Saji M, Fiorentino B, Reimold AM, Singer DS, Kohn LD 1998 Regulation of major histocompatibility class II gene expression in FRTL-5 thyrocyte: opposite effects of interferon and methimazole. Endocrinology 139: 290–302
32. Mitsiades N, Poulaki V, Tseleni-Balafouta S, Chrousos GP, Koutras DA 2000 Fas ligand expression in thyroid follicular cells from patients with thionamide-treated Graves' disease. Thyroid 10:527–532
33. Machia E, Nakai A, Janiga A, Sakurai A, Fisfaren ME, Gardner P, Soltani K, DeGroot LJ 1990 Characterization of site-specific polyclonal antibodies to c-erb A peptides recognizing human thyroid hormone receptors $\alpha 1$, $\alpha 2$, β and native 3,5,3′-triiodothyronine receptor, and study of tissue distribution of the antigen. Endocrinology 126:3232–3239
34. Tagami T, Nakamura H, Sasaki S, Mori T, Yoshioka H, Yoshida H, Imura H 1990 Immunohistochemical localization of nuclear 3,5,3′-triiodothyronine receptor proteins in rat tissues studied with antiserum against c-erb A/T3 receptor. Endocrinology 127:1727–1734
35. Bronnegard M, Torring O, Boos J, Sylven C, Marcus C, Wallin G 1994 Expression of thyrotropin receptor and thyroid hormone receptor messenger ribonucleic acid in normal, hyperplastic, and neoplastic human thyroid tissue. J Clin Endocrinol Metab 79:384–389
36. Lazarus JH, Marchant B, Alexander WD, Clark DH 1975 35-S-antithyroid drug concentration and organic binding of iodine in the human thyroid. Clin Endocrinol (Oxf) 4:609–615
37. Okamura Y, Shigemasa C, Tatsuhara T 1986 Pharmacokinetics of methimazole in normal subjects and hyperthyroid patients. Endocrinology 33:605–615
38. Cooper DS, Saxe VC, Meskell M, Maloof F, Ridgway EC 1982 Acute effects of propylthiouracil (PTU) on thyroidal iodine organization and peripheral iodothyronine deiodination: correlation with serum PTU levels measured by radioimmunoassay. J Clin Endocrinol Metab 54:101–107
39. McKenna NJ, Lanz RB, O'Malley BW 1999 Nuclear receptor coregulators: cellular and molecular biology. Endocr Rev 20:321–344
40. Cohen RN, Wondisford FE, Hollenberg AN 1998 Two separate NCoR (nuclear receptor corepressor) interaction domains mediate corepressor action on thyroid hormone response elements. Mol Endocrinol 12:1567–1581
41. Cohen RN, Putney A, Wondisford FE, Hollenberg AN 2000 The nuclear corepressors recognize distinct nuclear receptor complexes. Mol Endocrinol 14:900–914
42. Cohen RN, Brzostek S, Kim B, Chorev M, Wondisford FE, Hollenberg AN 2001 The specificity of interactions between nuclear hormone receptors and corepressors is mediated by distinct amino acid sequences within the interacting domains. Mol Endocrinol 15:1049–1061
43. Li X, Wong J, Tsai SY, Tsai MJ, O'Malley BM 2003 Progesterone and glucocorticoid receptors recruit distinct coactivator complexes and promote distinct patterns of local chromatin modification. Mol Cell Biol 23:3763–3773
44. Onate SA, Boonyaratanakornkit V, Spencer TE, Tsai SY, Tsai MJ, Edwards DP, O'Malley BW 1998 The steroid receptor coactivator-1 contains multiple receptor interacting and activation domains that cooperatively enhance the activation function 1 (AF1) and AF2 domains of steroid receptors. J Biol Chem 273:12101–12108
45. Mangelsdorf DJ, Evans RM 1995 The RXR heterodimers and orphan receptors. Cell 83:841–850

JCEM is published monthly by The Endocrine Society (http://www.endo-society.org), the foremost professional society serving the endocrine community.

Osteoporos Int (2006) 17: 105–108
DOI 10.1007/s00198-005-1923-3

ORIGINAL ARTICLE

High-dose glucocorticoid treatment induces rapid loss of trabecular bone mineral density and lean body mass

Koshi Natsui · Kiyoshi Tanaka · Michio Suda
Akihiro Yasoda · Yoko Sakuma · Ami Ozasa
Shoichi Ozaki · Kazuwa Nakao

Received: 11 December 2004 / Accepted: 5 April 2005 / Published online: 11 May 2005

Abstract A recent large-scale study revealed that glucocorticoid treatment increased fracture risk, which occurred at a far smaller dose and by a shorter duration than previously thought. To study the underlying mechanism for the increased risk of fracture, we studied the early changes in bone mineral density (BMD) and body composition by dual energy X-ray absorptiometry (DXA) after initiating high-dose glucocorticoid treatment. High-dose glucocorticoid treatment was arbitrarily defined as daily doses of ≥40 mg of a predonisolone equivalent. The 33 patients enrolled in this study had not received glucocorticoid treatment before. Only 2 months of treatment resulted in substantial BMD loss, most markedly in the lumbar spine, followed by the femoral neck and total body, which suggests the preferential trabecular bone loss. Body composition was also greatly affected. Thus, 2-month treatment with glucocorticoid significantly reduced bone mineral content (BMC), lean body mass (LBM) and increased fat mass (FAT). Our results are likely to have some clinical relevance. First, BMD loss occurs quite rapidly after starting glucocorticoid treatment, and patients receiving glucocorticoid treatment should be more carefully monitored for their BMD. Second, LBM, which mainly represents muscle volume, decreases rapidly after initiating glucocorticoid treatment. Decreased LBM might be also responsible for the increased risk of fracture, since falling is a well-known risk factor for fracture, and patients receiving glucocorticoid treatment should also be evaluated for their body composition.

Keywords Body composition · Dual energy X-ray absorptiometery · Glucocorticoid-induced osteoporosis · Lean body mass · Steroid myopathy

K. Natsui (✉)
Department of Medicine,
Fukui Red Cross Hospital, 4-2-1 Tsukimi,
918-8501 Fukui, Japan
E-mail: IBZ00745@nifty.ne.jp
Tel.: +81-776-363630
Fax: +81-776-364133

K. Tanaka
Department of Food and Nutrition,
Kyoto Women's University, Higashiyama,
Kyoto, Japan

M. Suda
Department of Endocrinology, Kyoto City Hospital,
Nakagyo, Kyoto, Japan

A. Yasoda · Y. Sakuma · A. Ozasa · K. Nakao
Department of Endocrinology and Metabolism,
Kyoto University Hospital, Sakyo, Kyoto, Japan

S. Ozaki
Division of Rheumatology and Allergy,
St. Marianna University School of Medicine,
Kawasaki, Japan

Introduction

Among the various adverse events associated with therapeutic glucocorticoid use, osteoporotic fracture is considered to be the most common complication [1]. A large-scale study from the UK clearly demonstrated that glucocorticoid treatment, even with small dosage and for short duration, significantly increased the risk of fracture [2]. Furthermore, a recent meta-analysis by van Staa et al. showed that the risk of fracture increased quite rapidly (within 3 to 6 months) after initiating the glucocorticoid treatment [3]. Prompted by these works, we have studied the early effects of high-dose glicocorticoid use on the skeletal system.

The purpose of this paper was twofold: first, to examine the initial effects of glucocorticoid on bone mineral density (BMD) at various skeletal sites; second, to study the effects of glucocorticoid on body composition based on the following considerations. Recent evidence suggests that the fracture threshold in patients with glucocorticoid-induced osteoporosis (GIO) is different from that in patients with primary osteoporosis [4]. Although glucocorticoid is known to cause muscle

weakness called "steroid myopathy" [5], far less attention has been paid to this condition than GIO. We suspected that myopathy and increased risk of falling might also be responsible for the increased risk of fracture. The patients included in this study received glucocorticoid treatment for the first time, and the patients that received higher doses of glucocorticoid were exclusively studied. The protocol was so determined because we considered that it is a suitable model to study the initial effects of high-dose glucocorticoid on the musculoskeletal system.

Materials and methods

Thirty-three patients hospitalized at the Kyoto University Hospital and scheduled to receive intensive glucocorticoid therapy were recruited in this study (Table 1). None of the patients had received glucocorticoid treatment before. Five patients were male (54.0 ± 7.6 years old), and 28 were female (38.9 ± 16.4 years old). "Intensive glucocorticoid therapy" was arbitrarily defined as the daily dose of glucocorticoid ≥40 mg of predonisolone equivalent. Nineteen patients received intravenous pulse treatment followed by oral glucocorticoid treatment. Fourteen patients received only oral glucocorticoid treatment. Their underlying diseases are as follows, with the number of subjects in parentheses: Graves' ophthamopathy (8), dermatomyositis (DM), polymyositis (PM) and mixed connective disorder (MCTD) (9), systemic lupus erythematodes (SLE) (16) and nephrotic syndrome (NS) [2]. Bone mineral density (BMD) and body composition were measured before and 2 months after initiating the glucocorticoid therapy. These measurements were performed with dual energy X-ray absorptiometry (DXA) (QDR-2000; Hologic, Waltham, Mass.) by a single examiner. BMDs were measured for the lumbar spine (L2–4), femoral neck and whole body. From the whole body measurement, the following parameters of body composition were obtained: lean body mass (LBM), fat mass (FAT) and bone mineral content (BMC).

Table 1 Patient characteristics

Number of patients	33		
Sex and age	Male	5	(54.0 ± 7.6 years old)
	Female	28	(38.9 ± 16.4 years old)
Underlying diseases	Systemic lupus erythematosus	(16)	
	Myositis	(9)	
	Graves' opthalmopathy	(8)	
Route of administration	Intravenous pulse + oral	(19)	
	Oral	(14)	

Results

High-dose glucocorticoid treatment for 2 months caused significant BMD loss at all three sites measured in the present study (Table 2). Of these three sites, the lumbar spine showed the greater percentage of BMD loss (–2.87%) compared to the femoral neck (–1.37%) and whole body (–1.10%). These differences were highly statistically significant by Fisher's PLSD.

The effect of high-dose glucocorticoid treatment on body composition was also studied (Table 3A). Two cases with nephrotic syndrome were excluded from the statistical analysis because the existence of severe edema is likely to interfere with the measurement of body composition. The initial body mass index (BMI) of the patients was 20.07 ± 3.06 kg/m^2, which did not significantly deviate from the standard BMI value of 22. Intensive glucocorticoid treatment for 2 months significantly decreased the BMI to 19.19 ± 2.83 kg/m^2 ($P < 0.05$).

BMC and LBM significantly decreased after glucocorticoid treatment (Table 3A). In contrast, fat mass (FAT) significantly increased. When expressed as %FAT, that is the ratio of FAT divided by body weight, the change was more pronounced. Thus, %FAT before treatment was 22.72 ± 6.22%, and it increased to 25.26 ± 5.65% after treatment ($P < 0.001$).

To exclude possible interference by the pre-existing myositis, data were also analyzed in 24 patients, excluding the cases with muscle involvement (DM/PM/MCTD) (Table 3B). The results were similar to the ones from the whole 33 cases. Thus BMI, BMC and LBM significantly decreased after the treatment. Although FAT after treatment was not statistically different from the pre-treatment value, %FAT after treatment was significantly higher than that before treatment.

The total dosage of glucocorticoid within 2 months ranged from 1,000 to 4,000 mg in cases with oral glucocorticoid treatment, and from 4,500 to 12,000 mg in cases with intravenous pulse treatment. Total glucocorticoid dosage correlated with none of the parameters in the present study, such as BMI, LBM and fat mass (data not shown).

Discussion

Recently, van Staa et al. clearly demonstrated that glucocorticoid use is a significant risk factor for both vertebral and nonvertebral fractures [2]. Their study is an exceptionally large-scale study from the UK including over 240,000 subjects in both control and glucocorticoid groups. Their reports have some important clinical implications. First, they found that even a small dosage of glucocorticoid use for a short duration of time significantly increased the risk of fracture. Until recently, glucocorticoid use was considered to be a risk factor for osteoporosis when the average daily dosage was greater

Table 2 Changes in bone mineral density after 2 months of high-dose glucocorticoid treatment

	Pretreatment	Post-treatment	*P* value
Lumbar spine (L2–4)	0.94±0.17	0.91±0.17	<0.0001
Femoral neck	0.735±0.123	0.725±0.125	<0.01
Whole body	1.031±0.111	1.019±0.111	<0.001

than or equal to the predonisolone equivalent of 7.5 mg and the duration was >6 months [6]. According to van Staa et al., however, fracture risk was already increased at as early as 3 months after starting the glucocorticoid treatment, and even a daily dosage of less than 2.5 mg predonisolone equivalent was associated with increased risk of vertebral fracture [2]. Another important implication was that glucocorticoid treatment was unequivocally proven to be a risk factor for fracture. The current concept holds that the reduction of fracture risk should be the endpoint in the treatment of osteoporosis, the increase of BMD being only a surrogate endpoint [7]. Thus, it is a landmark study in that fracture was the endpoint in the study of GIO.

In the current study, only 2 months of high-dose glucocorticoid treatment markedly decreased BMD in all three sites measured: the lumbar spine, femoral neck and whole body. The BMD decrease was the greatest in the lumbar spine compared to the femoral neck and whole body. These differences are likely to be due to the variable composition of each bone [8]. Thus, the lumbar spine is mainly composed of trabecular bone, and both cortical and trabecular bones contribute to the femoral neck BMD. Since approximately 70% of total bone volume is composed of cortical bone, cortical bone volume is the major determinant of total body BMD. Therefore, these results suggest that trabecular bone is mainly affected by intensive glucocorticoid treatment, which is in accordance with the previous reports [6].

Although glucocorticoid affects various aspects of skeletal homeostasis, its major effect is considered to be the suppression of bone formation, which is mainly exerted through inducing apoptosis in osteoblasts and osteocytes, and suppressing local IGF-1 production [9, 10]. Although glucocorticoid is known to decrease intestinal calcium absorption, the effect is usually only modest and does not cause marked secondary hyperparathyroidism. Glucocorticoid also increases urinary calcium excretion by inhibiting tubular calcium reabsorption. With regard to bone resorption, glucocorticoid treatment is reported to enhance bone resorption transiently by inducing RANKL and suppressing OPG [9, 10].

Despite the significant detrimental effects of glucocorticoid on BMD, it is not likely to be the sole explanation for the glucocorticoid-induced increase in the fracture rate. The fracture risk in GIO has been reported to be either altered [11] or unaltered [12]. A recent paper by Wallch, however, strongly favors the notion that fracture occurs at higher BMD values in GIO than in postmenopausal osteoporosis [4]. In their report, which is part of the risedronate trial on GIO, the vertebral fracture rate was as high as 16%, whereas lumbar BMD was only modestly decreased, the average T score being −1.2. Van Staa et al. suggested three mechanisms for the increased fracture rate in GIO [2]: the apoptosis of osteoblasts and osteocytes, the marked alteration in bone turnover and non-skeletal mechanisms such as falling. Glucocorticoid is known to alter the body composition greatly. Muscle weakness called "steroid myopathy" and central obesity are well-known complications of glucocorticoid treatment [5], and muscle weakness is by no doubt one of the major risk factors of falling. In this study, body composition was evaluated by DXA, since it is considered to be a standard method for the evaluation of body composition as well as for BMD measurement [13]. LBM significantly decreased, and FAT increased in a reciprocal fashion in within only 2 months, Therefore, the percentage of fat (%FAT) increased by approximately 10%. Although vertebral fracture, which is the most prevalent fracture in GIO, is not associated with falling [10], an increased rate of falling would lead to the increased risk of hip and wrist fractures. Thus, our current finding may explain at least partially the increased fracture risk in glucocorticoid treatment.

Another implication of the current findings would be the rapidity with which bone loss occurs after initiating

Table 3 Changes in body composition after 2 months of high-dose glucocorticoid treatment. *A* and *B* show the data from whole subjects and data from patients excluding ones with myositis, respectively. BMC, LBM and FAT are expressed in kg. %FAT is the ratio of fat to body weight

	Pretreatment	Post-treatment	*P* value
A			
Body mass index (BMI)	20.07±3.06	19.19±2.83	<0.05
Body composition			
Bone mineral content (BMC)	1.94±0.38	1.88± 0.37	<0.001
Lean body mass (LBM)	37.30±6.80	34.26± 5.00	<0.0001
Fat mass (FAT)	11.66±4.00	12.47±3.95	<0.05
%FAT	22.72±6.22	25.26±5.65	<0.001
B			
Body mass index (BMI)	20.00±3.37	19.28±3.05	<0.05
Body composition			
Bone mineral content (BMC)	1.89±0.34	1.84±0.33	<0.001
Lean body mass (LBM)	35.52±6.37	33.33±4.79	<0.005
Fat mass (FAT)	12.03±4.51	12.44±4.22	NS
% FAT	23.89±6.75	25.60±6.22	<0.05

intensive glucocorticoid treatment. It is now established that even low dose glucocorticoid treatment increases the fracture risk. Vestergaard et al. reported that even a limited daily dose of glucocrticoid (more than an average dose of 71 μg predonisolone per day) was associated with an increased risk of hip fracture [14]. In the guideline for GIO recently published by the UK, it is recommended that BMD measurement should be considered for patients committed or exposed to oral glucocorticoid for more than 3 months, irrespective of the glucocorticoid dose [15]. These reports, together with the current findings, strongly suggest that attention should be paid to the prevention as well as the treatment of GIO.

These changes are unlikely to be secondary to hospitalization or due to underlying disease alone. First, increased %FAT in face of decreased body weight is quite unlikely to occur as the result of underlying disease or the subsequent malnutrition. Moreover, when the subgroup of patients with euthyroid Graves' disease was separately analyzed, these changes in body composition and biochemical parameters were similarly observed (data not shown). These patients have inflammatory changes only in their extraocular muscle and do not have any limitation in their daily activities except for double vision. Therefore, these marked changes are probably due to the intensive glucocorticoid treatment rather than other factors. Additionally, the patients' BMD was not markedly decreased before treatment. Since reference data for whole body BMD using QDR-2000 in the Japanese population is not available, we have not expressed our data in Z score. The young adult mean (YAM) for lumbar spine BMD in Japanese women is 1.011 ± 0. The YAM for the femoral neck BMD is 0.787 ± 0.109 for women and 0.863 ± 0.127 for men. Thus, it is quite unlikely that underlying diseases had adversely affected the subjects' skeletons before glucocorticoid treatment.

In summary, we have shown that intensive glucocorticoid treatment rapidly induces trabecular bone loss and lean body mass, both of which probably contribute to the recently reported rapid onset of increased fracture risk after initiating glucocorticoid treatment.

References

1. Saag KG, Koehnke R, Caldwell JR, Brasington R, Burmeister LF, Zimmerman B, Kohler JA, Furst DE (1994) Low dose long-term corticosteroid therapy in rheumatoid arthritis: an analysis of serious adverse events. Am J Med 96:115–123
2. van Staa TP, Leufkens HGM, Abenhaim L, Zhang B, Cooper C (2000) Use of oral corticosteroid and risk of fractures. J Bone Miner Res 15:993–1000
3. van Staa TP, Leufkens HG, Cooper C (2002) The epidemiology of corticosteroid-induced osteoporosis: a meta-analysis. Osteoporos Int 13:777–787
4. Wallach S, Cohen S, Reid DM, Hughes RA, Hosking DJ, Laan RF, Doherty SM, Maricic M, Rosen C, Brown J, Barton I, Chines AA (2000) Effects of risedronate treatment on bone density and vertebral fracture in patients on corticosteroid therapy. Calcif Tissue Int 67:277–285
5. Kanda F, Okuda S, Matsushita T, Takatani K, Kimura KI, Chihara K (2001) Steroid myopathy: pathogenesis and effects of growth hormone and insulin-like growth factor-I administration. Horm Res 56:S24–S28
6. American College of Rheumatology Task Force on Osteoporosis Guidelines (1996) Recommendations for the prevention and treatment of glucocorticoid-induced osteoporosis. Arth Rheum 39:1791–1801
7. Pearson D, Miller CG (eds) (2002) Clinical trials in osteoporosis. Springer, Heidelberg Germany New York
8. Bonnick SL, Lewis LA (2002) Bone densitometry for technologists. Humana Press, Totowa, NJ
9. Canalis E, Giustina A (2001) Glucocorticoid-induced osteoporosis: summary of a workshop. J Clin Endocrinol Metab 86:5681–5685
10. Canalis E, Delany AM (2002). Mechanism of glucocorticoid action in bone. Ann NY Acad Sci 966:73–81
11. Luengo M, Picado C, Del Rio L, Guanabens N, Monsterrat JM, Setoain J (1991) Vertebral fractures in steroid dependent asthma and involutional osteoporosis. Thorax 46:803–806
12. Selby PL, Halsey JP, Adams KRH, Klimiuk P, Knight SM, Pal B, Stewart IM, Swinson DR (2000) Corticosteroids do not alter the threshold for vertebral fracture. J Bone Miner Res 15:952–956
13. Houtkooper LB, Going SB, Sproul J, Blew RM, Lohman TG (2000) Comparison of methods for assessing body-composition changes over 1 year in postmenopausal women. Am J Clin Nutr 72:401–406
14. Vestergaard P, Olsen ML, Paaske Johnsen S, Rejnmark L, Toft Sorensen H, Mosekilde L. (2003) J Intern Med 254:486–493
15. Bone and Tooth Society, National Osteoporosis Society, Royal College of Physicians. (2002) Glucocorticoid-induced osteoporosis: guidelines for prevention and treatment. Royal College of Physicians, London

Original Article

Blockade of Pancreatic Islet–Derived Ghrelin Enhances Insulin Secretion to Prevent High-Fat Diet–Induced Glucose Intolerance

Katsuya Dezaki,[1] Hideyuki Sone,[1] Masaru Koizumi,[1,2] Masanori Nakata,[1] Masafumi Kakei,[3] Hideo Nagai,[2] Hiroshi Hosoda,[4] Kenji Kangawa,[4] and Toshihiko Yada[1]

The gastric hormone ghrelin and its receptor, growth hormone secretagogue receptor (GHSR), are expressed in pancreas. Here, we report that ghrelin is released from pancreatic islets to regulate glucose-induced insulin release. Plasma concentrations of ghrelin, as well as insulin, were higher in pancreatic veins than in arteries. GHSR antagonist and immunoneutralization of endogenous ghrelin enhanced glucose-induced insulin release from perfused pancreas, whereas exogenous ghrelin suppressed it. GHSR antagonist increased plasma insulin levels in gastrectomized and normal rats to a similar extent. Ghrelin knockout mice displayed enhanced glucose-induced insulin release from isolated islets, whereas islet density, size, insulin content, and insulin mRNA levels were unaltered. Glucose tolerance tests (GTTs) in ghrelin knockout mice showed increased insulin and decreased glucose responses. Treatment with high-fat diet produced glucose intolerance in GTTs in wild-type mice. In ghrelin knockout mice, the high-fat diet–induced glucose intolerance was largely prevented, whereas insulin responses to GTTs were markedly enhanced. These findings demonstrate that ghrelin originating from pancreatic islets is a physiological regulator of glucose-induced insulin release. Antagonism of the ghrelin function can enhance insulin release to meet increased demand for insulin in high-fat diet–induced obesity and thereby normalize glycemic control, which may provide a potential therapeutic application to counteract the progression of type 2 diabetes. *Diabetes* 55:3486–3493, 2006

From the [1]Division of Integrative Physiology, Department of Physiology, Jichi Medical University School of Medicine, Shimotsuke, Tochigi, Japan; the [2]Department of Surgery, Jichi Medical University School of Medicine, Shimotsuke, Tochigi, Japan; the [3]Department of Internal Medicine, Division of Endocrinology, Diabetes and Geriatric Medicine, Akita University School of Medicine, Akita, Japan; and the [4]Department of Biochemistry, National Cardiovascular Center Research Institute, Osaka, Suita, Japan.

Address correspondence and reprint requests to Toshihiko Yada, Division of Integrative Physiology, Department of Physiology, Jichi Medical University School of Medicine, Yakushiji 3311-1, Shimotsuke, Tochigi 329-0498, Japan. E-mail: tyada@jichi.ac.jp.

Received for publication 28 June 2006 and accepted in revised form 6 September 2006.

ELISA, enzyme-linked immunosorbent assay; GHRP, growth hormone releasing peptide; GHSR, growth hormone secretagogue receptor; GTT, glucose tolerance test; HKRB, HEPES-added Krebs-Ringer bicarbonate buffer; ITT, insulin tolerance test.

DOI: 10.2337/db06-0878

Ghrelin, an acylated 28–amino acid peptide, was isolated from the stomach as the endogenous ligand (1) for the growth hormone secretagogue receptor (GHSR) (2). Circulating ghrelin is produced predominantly in the stomach (3). Ghrelin potently stimulates growth hormone release and feeding and exhibits positive cardiovascular effects, suggesting a possible clinical application of ghrelin (4). Ghrelin inhibits insulin release in mice, rats, and humans (5–8). Low plasma ghrelin levels are associated with elevated fasting insulin levels and insulin resistance (9,10). These findings suggest both physiological and pathophysiological roles for ghrelin in insulin release.

Although the nutritional, endocrine, and neural regulation of insulin release has been well characterized, much less is known about its autoregulation within islets. Ghrelin and GHSR are also located in pancreatic islets (8,11–15). We previously reported that in isolated islets, GHSR blockade and antiserum against acylated ghrelin markedly enhanced glucose-induced increases in insulin release and cytosolic Ca^{2+} concentration in islets (8). Although exogenous ghrelin suppressed insulin release, this effect required a concentration of 10 nmol/l, which is higher than the circulating ghrelin levels (16,17). These findings suggest that ghrelin at relatively high concentrations achieved within islets, rather than the circulating ghrelin, may regulate insulin secretion. The current study examined whether ghrelin originating from pancreatic islets could regulate insulin release and whether manipulation of ghrelin could affect glucose intolerance associated with obesity. We show here that ghrelin is released from pancreatic islets to downregulate glucose-induced insulin release and that ghrelin knockout mice escape high-fat diet–induced glucose intolerance because of enhanced insulin release.

RESEARCH DESIGN AND METHODS

Male Wistar rats (Japan SLC, Hamamatsu, Japan), ghrelin knockout mice, and wild-type C57BL/6J mice (Charles River Laboratories Japan, Yokohama, Japan) were housed in accordance with our institutional guidelines and with the Japanese Physiological Society's guidelines for animal care. Ghrelin knockout mice were the kind gift of Drs. T. Sato and M. Kojima (Kurume University). In these mice, the whole ghrelin gene sequence has been deleted. Animals were backcrossed with the C57B6/J strain for at least six generations. Proper deletion of the ghrelin gene was confirmed by Southern and Northern blot analysis. Total gastrectomy in 6-week-old male Wistar rats was carried out by resecting the stomach, followed by anastomosis of the cut edge of the

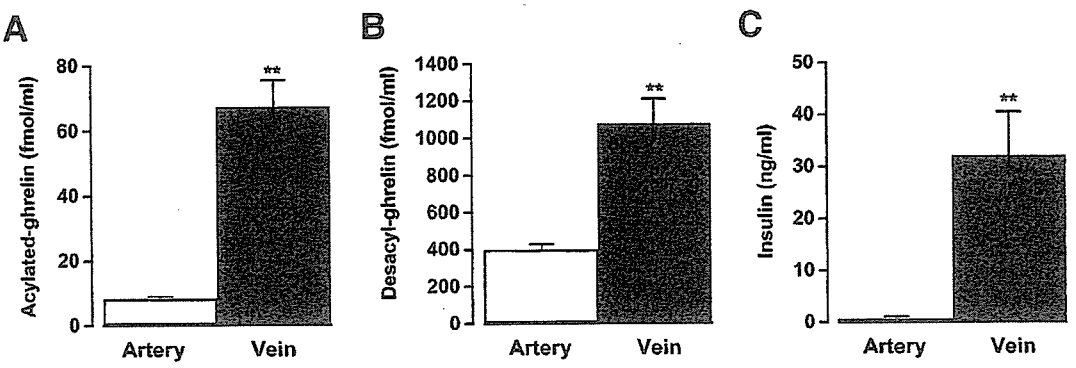

FIG. 1. Acylated ghrelin (*A*) and desacyl-ghrelin (*B*), as well as insulin (*C*), were present at higher concentrations in the pancreatic vein (splenic vein) than in the pancreatic artery (celiac artery) in rats (n = 8). **P < 0.01 vs. artery.

esophagus and the upper jejunum 4 cm distal to the Treitz ligament. At 2 months after surgery, gastrectomized rats were used for experiments.

Measurements of plasma insulin and ghrelin concentrations. Ghrelin (Peptide Institute, Osaka, Japan) and [D-Lys^3]-growth hormone releasing peptide-6 ([D-Lys^3]GHRP-6; Sigma-Aldrich, St. Louis, MO) were administered intraperitoneally to male Wistar rats (8 weeks old) or gastrectomized rats (3 months old) after overnight fasting. Blood was obtained from tails, and plasma insulin concentrations were measured using an enzyme-linked immunosorbent assay (ELISA) kit (Morinaga Institute of Biological Science, Yokohama, Japan). To measure plasma ghrelin concentrations, blood samples were collected from the pancreatic arteries (celiac artery) and veins (splenic vein) and portal veins of anesthetized rats or mice. To avoid inflow of ghrelin from intestine and stomach to the splenic vein, the inferior mesenteric vein and spleen side of the splenic vein—including the short gastric and left gastro-omental veins—were ligated. Plasma concentrations of acylated ghrelin and desacyl-ghrelin were measured using ELISA kits (Mitsubishi Kagaku Iatron, Tokyo, Japan).

Morphological analysis of pancreatic islets in wild-type and ghrelin knockout mice. Pancreata from male wild-type and ghrelin knockout mice were fixed in 4% paraformaldehyde, and two to three random sections were generated per mouse pancreas. Three mice were studied in each genotype. The sections were incubated overnight with mouse monoclonal anti-insulin antibodies (Sigma-Aldrich) at dilutions of 1:1,000 at 4°C. Samples were then incubated in Alexa Fluor 488–labeled goat anti-mouse IgG (Molecular Probes, Eugene, OR). Immunofluorescence for insulin was observed with photomultipliers of a multiphoton laser-scanning microscope (FluoView FV300-TP; Olympus, Tokyo, Japan). Islet number per unit area of pancreas and islet size were measured.

Measurements of insulin release in islets. Islets of Langerhans were isolated by collagenase digestion from male ghrelin knockout and wild-type (C57BL/6J) mice as previously reported (8,18), with slight modifications. Animals were anesthetized by intraperitoneal injection of pentobarbitone at 80 mg/kg, and collagenase at 1.05 mg/ml (Sigma-Aldrich) was injected into the common bile duct. Collagenase was dissolved in 5 mmol/l Ca^{2+}-containing HEPES-added Krebs-Ringer bicarbonate buffer (HKRB) solution (in mmol/l: 129 NaCl, 5.0 $NaHCO_3$, 4.7 KCl, 1.2 KH_2PO_4, 2.0 $CaCl_2$, 1.2 $MgSO_4$, and 10 HEPES, pH 7.4, with 0.1% BSA). Pancreata were dissected and incubated at 37°C for 16 min. Islets were collected and used for insulin release experiments. Groups of 12–15 islets were incubated for 1 h in HKRB at 37°C with 2.8 mmol/l glucose for stabilization, followed by test incubation for 1 h in HKRB with 2.8, 8.3, or 16.7 mmol/l glucose. Insulin concentrations were determined by an ELISA kit (Morinaga Institute of Biological Science).

Real-time RT-PCR analysis. Total RNA of islets was isolated using TRIzol (Invitrogen, Carlsbad, CA) and treated with RQ1-DNase (Promega, Madison, WI) to remove residual contaminations with DNA. First-strand cDNA synthesis was completed using ReverTra Ace (Toyobo, Osaka, Japan). Primers for real-time PCR were first examined by HotStarTaq DNA polymerase (94°C for 15 s, 55°C for 20 s, and 72°C for 20 s × 30 cycles; Qiagen, Hilden, Germany) and agarose gel electrophoresis for correct product size and absence of primer-dimer formation. Using a QuantiTect SYBR Green PCR kit, real-time PCRs (95°C for 15 s, 55°C for 20 s, and 72°C for 20 s × 35 cycles) were performed in an ABI-Prism 7700 sequence detector (Applied Biosystems, Foster City, CA). Product accumulation was measured in real time, and the mean cycle threshold (Ct; the cycle during which product is first detected) was determined for replicate samples (n = 5 independent reactions per primer pair and cDNA sample) run on the same plate. Different cDNA samples were normalized using primer sets to the housekeeping gene β-actin. Primers were as follows: β-actin, 5′-TTCCCCTCCATCGTGGGCCGC-3′ and 5′-GATGGCTACGTACATGGCTGG-3′; Insulin 1, 5′TAGTGACCAGCTATAATCAGAG-3′ and 5′-ACGCCAAGGTCTGAAGGTCC-3′; and Insulin 2, 5′-CCCTGCTGGCCCTGCTCTT-3′ and 5′-AGGTCTGAAGGTCACCTGCT-3′.

In vitro perfusion of the pancreas. Pancreata were perfused using a modification of the method of Grodsky and Fanska (19). Pancreata were isolated with segments of the duodenum and spleen. An arterial cannula was introduced into the celiac artery, and a venous cannula was inserted into the portal vein. The baseline perfusate consisted of HKRB (pH 7.4) containing 2.8 mmol/l glucose, 0.5% BSA, and 4% Dextran T70. The perfusate, maintained at 37°C, was continually oxygenated in an atmosphere of 95% O_2/5% CO_2. After a 20-min preincubation period, each pancreas was perfused for 10 min with the baseline perfusate. Pancreata were then perfused for 30 min with 8.3 mmol/l glucose or 8.3 mmol/l glucose with test reagents. The flow rate was maintained at 2.5 ml/min throughout measurements. Fractions, collected in chilled tubes at 1-min intervals, were stored at −20°C until assayed for immunoreactive insulin.

Glucose tolerance tests and insulin tolerance tests. In glucose tolerance test (GTT) studies, 2 g/kg glucose was injected intraperitoneally into mice, followed by blood sampling from the tail vein. In insulin tolerance test (ITT) studies, insulin (0.75 units/kg) was injected intraperitoneally, followed by collection of blood samples from the tail vein. Blood glucose concentrations were measured using a GlucoCard DIA meter (Arkray, Kyoto, Japan), while insulin concentrations were determined using an ELISA kit (Morinaga Institute of Biological Science).

Statistical analysis. Data are the means ± SE. Statistical analyses were performed using Student's t test or one-way ANOVA. $P < 0.05$ was considered statistically significant.

RESULTS

Release of ghrelin from pancreas. Ghrelin is expressed in the pancreatic islets (8,11–15). Release of ghrelin from pancreatic islets was assessed by comparing the ghrelin level in the pancreatic vein (splenic vein) with that in the pancreatic artery (celiac artery) in anesthetized rats. The concentrations of both acylated ghrelin and desacyl-ghrelin in the pancreatic vein were significantly higher (about eight times and three times, respectively) than those in the pancreatic artery in rats (Fig. 1*A* and *B*). The concentration of insulin was significantly higher in the pancreatic vein than in the pancreatic artery (Fig. 1*C*).

Endogenous ghrelin inhibits insulin release in perfused pancreas. Our previous in vitro study showed that GHSR antagonists and anti-ghrelin antiserum enhanced glucose-induced insulin release in isolated rat islets (8), suggesting an insulinostatic action of islet-originated ghrelin. To establish a physiological function of endogenous ghrelin in islets, we studied insulin release using perfused rat pancreas, which retains well intact islet circulation. A rise in the perfusate glucose concentration from 2.8 to 8.3 mmol/l evoked insulin release in a biphasic manner (Fig. 2*A*). The first and second phases of glucose-induced